SOCIETÀ TOSCANA
DI
Scienze Naturali
RESIDENTE IN PISA

ATTI
DELLA
SOCIETÀ TOSCANA
DI
SCIENZE NATURALI

MEMORIE • SERIE A • VOLUME CXXVI • ANNO 2019

Edizioni ETS

INDICE - *CONTENTS*

P. Fulignati, P. Marianelli, A. Sbrana – Quantitative SEM-EDS analysis of reference silicate mineral and glass samples.
Analisi quantitative SEM-EDS di campioni di riferimento di vetri e minerali silicatici. pag. 5

G. Gallello, J. Bernabeu, A. Diez-Castillo, P. Escriba, A. Pastor, M. Lezzerini, S. Chenery, M.E. Hodson, D. Stump – Developing REE parameters for soil and sediment profile analysis to identify Neolithic anthropogenic signatures at Serpis Valley (Spain).
Sviluppo di parametri REE per l'analisi del profilo del suolo e dei sedimenti per identificare le firme antropogeniche neolitiche nella valle del Serpis (Spagna). » 13

D. Mauro, C. Biagioni, M. Pasero, H. Skogby – Crystal-chemistry of sulfates from the Apuan Alps (Tuscany, Italy). III. Mg-rich sulfate assemblages from the Fornovolasco mining complex.
Cristallochimica dei solfati delle Alpi Apuane (Toscana, Italia). III. Associazioni a solfati ricchi in Mg dal complesso minerario di Fornovolasco. » 33

P. Orlandi, M. D'Orazio – Cinnabar and other high-density minerals from stream sediments of Monti Pisani (Pisa and Lucca provinces, Tuscany).
Cinabro ed altri minerali ad elevata densità negli "stream sediments" dei Monti Pisani (Province di Lucca e Pisa, Toscana). » 45

M. Bacci, S. Corsi, L. Lombardi, M. Giunti – Gli interventi di ripristino morfologico ed ecologico del sistema dunale del Golfo di Follonica (Toscana, Italia): tecniche utilizzate e risultati del monitoraggio.
Morphological and ecological activities to restore the dune system at the Follonica Gulf (Tuscany, Italy): techniques used and monitoring results. » 57

D. Magaldi – Interglacial Pleistocene paleosols supporting old roads in central Tuscany.
Paleosuoli del Pleistocene interglaciale a supporto di antiche strade nella Toscana centrale. » 67

V. Spadini – Pliocene scleractinians from Estepona (Malaga, Spain).
Sclerattiniari pliocenici di Estepona (Malaga, Spagna). » 75

R. Giannecchini, M. Ambrosio, A. Del Sordo, M-T. Fagioli, A. Sartelli, Y. Galanti – Hydrogeological numerical modeling of the southeastern portion of the Lucca Plain (Tuscany, Italy), stressed by groundwater exploitation.
Modello idrogeologico numerico del settore sud-orientale della Piana di Lucca (Toscana, Italia) caratterizzato da sfruttamento intensivo delle risorse idriche. » 95

W. Landini – In memoria di Marco Tongiorgi (1934-2019).
In memory of Marco Tongiorgi (1934-2019). » 111

Processi Verbali della Società Toscana di Scienza Naturali residente in Pisa. Anno 2019 - http://www.stsn.it. » 121

Atti Soc. Tosc. Sci. Nat., Mem., Serie A, 126 (2019)
pagg. 13-32, figg. 4; tabb. 7; *doi: 10.2424/ASTSN.M.2019.09*

Gianni Gallello [1,2,3], Joan Bernabeu [3], Agustin Diez-Castillo [3], Pilar Escriba [3], Agustin Pastor [4], Marco Lezzerini [5], Simon Chenery [6], Mark E. Hodson [2], Daryl Stump [1,2]

DEVELOPING REE PARAMETERS FOR SOIL AND SEDIMENT PROFILE ANALYSIS TO IDENTIFY NEOLITHIC ANTHROPOGENIC SIGNATURES AT SERPIS VALLEY (SPAIN)

Abstract - G. Gallello, J. Bernabeu, A. Diez-Castillo, P. Escriba, A. Pastor, M. Lezzerini, S. Chenery, M.E. Hodson, D. Stump, *Developing REE parameters for soil and sediment profile analysis to identify Neolithic anthropogenic signatures at Serpis Valley (Spain).*

In this study, patterns of rare earth elements (REE) have been developed and applied for the first time to sediments and soils to identify anthropogenic or natural layers in profiles sampled at several Neolithic settlements in the Serpis Valley area (Alicante, Spain). Most of these sites are characterized by dark brown paleosols that are easily distinguishable from the light brown paleosols of the valley. To demonstrate whether these strata are anthropogenic or natural requires a better geochemical understanding of sediment. Soil samples were taken across six different sites; four sites are associated with archaeological findings (sites BF, LP, PB and AC8); another one is from a natural section from Mas D'Is (MD) located close to the archaeological site in which evidence of human occupation from the Neolithic period has been found; and the last corresponds to a place of uncertain attribution (BK5), where no archaeological remains have been found, but where layers of a recent agricultural activity are present. REE results comprising REE ratios, cerium and europium anomalies, and La/Yb-Sm/Eu correlations were compared with major and minor chemical components, mineralogical properties of the soil layers and, when it was possible, cross-referenced with archaeological data to aid interpretation. The results demonstrate the potential of REE data to distinguish strata associated with Neolithic occupation from those that have not been subjected to anthropogenic modification.

Keywords - rare earth elements, ICP-MS, archaeological deposits, anthropogenic layers, past settlements

Riassunto - G. Gallello, J. Bernabeu, A. Diez-Castillo, P. Escriba, A. Pastor, M. Lezzerini, S. Chenery, M.E. Hodson, D. Stump, *Sviluppo di parametri REE per l'analisi del profilo del suolo e dei sedimenti per identificare le firme antropogeniche neolitiche nella valle del Serpis (Spagna).*

In questo studio, le terre rare (REE) di sedimenti e suoli sono state utilizzate per la prima volta per identificare strati antropogenici o naturali in profili campionati in diversi insediamenti neolitici nell'area della valle del Serpis (Alicante, Spagna). La maggior parte di questi siti sono caratterizzati da paleosol marrone scuro che sono facilmente distinguibili dai paleosol marrone chiaro della valle. Per dimostrare se questi strati sono antropogenici o naturali è necessaria una migliore comprensione geochimica dei sedimenti. Sono stati prelevati campioni di terreno da sei siti diversi; quattro siti sono associati a reperti archeologici (siti BF, LP, PB e AC8); un altro proviene da una sezione naturale di Mas D'Is (MD) situata vicino al sito archeologico in cui sono state trovate prove dell'occupazione umana dal periodo neolitico; e l'ultimo corrisponde a un luogo di incerta attribuzione (BK5), dove non sono stati trovati resti archeologici, ma dove sono presenti strati di una recente attività agricola. I risultati di REE comprendenti rapporti REE, anomalie di cerio ed europio e correlazioni La/Yb - Sm/Eu sono stati confrontati con componenti chimici maggiori e minori, proprietà mineralogiche degli strati del suolo e, quando è stato possibile, riferimenti incrociati con dati archeologici per aiutare interpretazione. I risultati dimostrano il potenziale dei dati REE per distinguere gli strati associati all'occupazione neolitica da quelli che non sono stati sottoposti a modifiche antropogeniche.

Parole chiave - terre rare, ICP-MS, depositi archeologici, strati antropogenici, insediamenti del passato

Introduction

This study explores the use of rare earth elements (REE) to distinguish sediments and soils associated with human occupation from those that have not been subject to anthropogenic modification, taking the important Neolithic landscape of the Serpis Valley as its case-study. Perfecting this technique will have important implications for archaeologists and soil scientists because rare earth elements (REE) can act as a 'fingerprint' for particular sediments and soils, and as a consequence have been employed in a variety of different archaeological scenarios in order to identify past human activities (Cook *et al.*, 2006 ; Kamenov *et al.*, 2009; Saiano & Scalenghe, 2009; Nielsen & Kristiansen, 2014; Pastor *et al.*, 2016). These include studies by Gallello *et al.* (2013; 2014) that compared the REE signatures of strata at the Neolithic site of Mas d'Is, Spain, in order to test whether strata previously classified as natural or anthropogenic could be distinguished depending on their REE profile (the term 'anthropogenic' is used in our study very broadly to refer

[1] Department of Archaeology, University of York, King's Manor, York, YO17EP, UK
[2] Department of Environment and Geography, University of York, Wentworth Way Heslington, York, YO105NG, UK
[3] Department of Prehistory, Archaeology and Ancient History, University of Valencia, Avda. Blasco Ibáñez 28, 46010 Valencia, Spain
[4] Department of Analytical Chemistry, University of Valencia, 50 Dr. Moliner Street, 46100 Burjassot, Valencia, Spain
[5] Department of Earth Sciences, University of Pisa, Via S. Maria 53, 56126 Pisa, Italy
[6] British Geological Survey Environmental Science Centre, Nicker Hill Keyworth (Nottingham) NG125GG, UK
Corresponding author: Gianni Gallello (gianni.gallello@york.ac.uk)

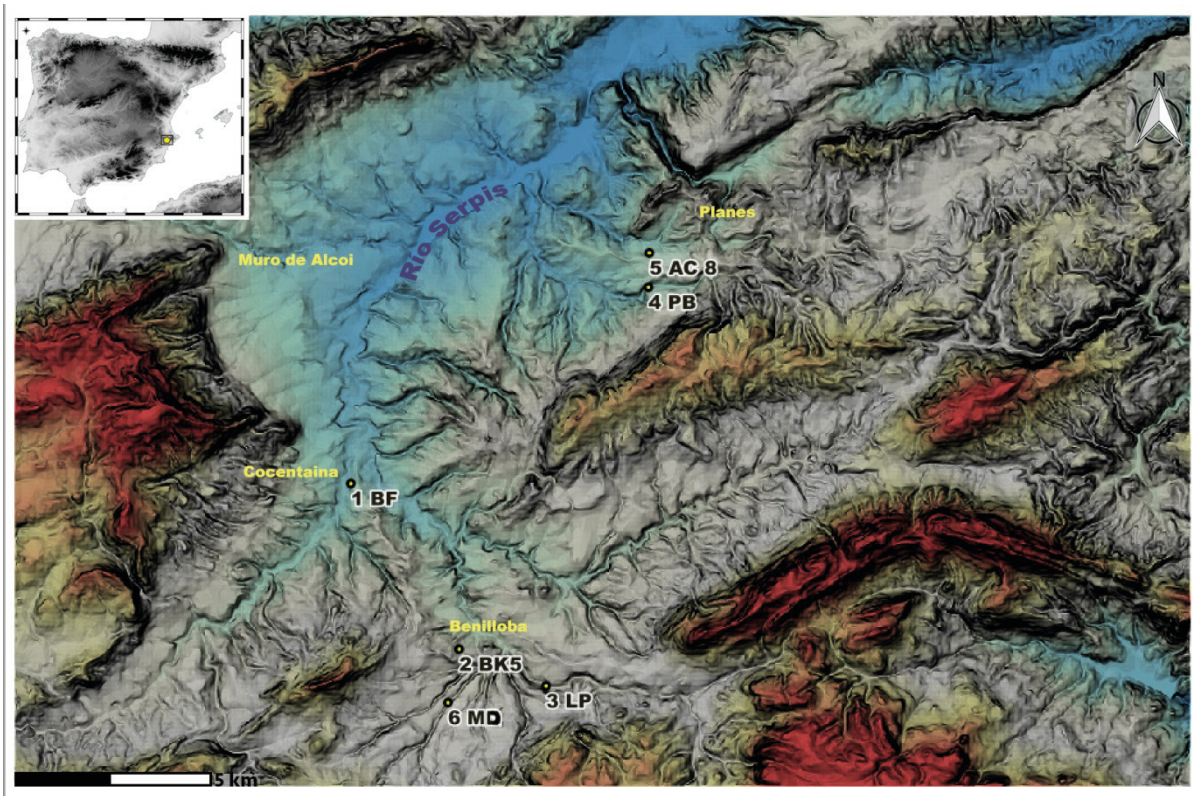

Figure 1. Location of the studied sections in Serpis Valley (Alicante, Spain). Note: colours mark the lowest (blue or light grey in grey tones) and highest (red or dark grey in grey tones) elevations on the map. MD: latitude 38.684742, longitude -0.399689 (584 m asl). AC8: latitude 38.785514, longitude -0.337122 (440 m asl). PB: latitude 38.777485, longitude -0.338284 (466 m asl). LP: latitude 38.687351, longitude -0.370126 (588 m asl). BF: latitude 38.735011, and longitude -0.426013 (426 m asl). BK5: latitude 38.696793, longitude -0.395943(541 m asl).

to any human activity that can impact the chemistry of soils and sediments). The same authors found that the use of major, minor and some trace elements was not sufficient to determine differences between archaeological layers in some sedimentological contexts.

The current study aims to test the capability of La/Yb-Sm/Eu correlations to distinguish between different sediments and soils and extends the use of REE normalized ratios and the examination of Ce and Eu anomalies used during the preliminary studies (Gallello *et al*., 2013; 2014) by examining soils across the entire Serpis Valley, in which Mas d'Is is located. In doing so, we aim to establish a new methodological approach for the identification of anthropogenic units in excavated cross-sections through REE analysis of soils and sediments.

Area description

The Upper and Middle Serpis Valley (also known as Valls d'Alcoi) is an area characterized by a typical Mediterranean drainage of the Iberian Peninsula (short and steep flow water-courses) that encompasses an area of around 1000 km^2 upstream of the Beniarrés dam. The main river (Serpis) follows a NE direction marked by the structure of the Valencian Baetic system (Diez-Castillo *et al*., 2007). The central depression (a horst) is filled by probably marine marls (Roca-Cervigón, 1991), characterized by several pediments varying between 700 m deep in the north area and 300 m in the south (Marco-Molina, 1990). The surrounding limestone mountains have summits of almost 1400 m.

Previous Mas d'Is archaeological fieldwork revealed different kinds of structures and layers dated from the earliest Neolithic period in the region up to the present times. Most of these archaeological features and strata are related to the Early and Middle Neolithic, including ditches, houses and open areas of diverse use, ranging in date from c. 5600 to 4000 BC (Bernabeu *et al*., 2003). The stratigraphic sequence filling these ditches shows the presence of paleosols that formed at different times during the Neolithic. Moreover, field survey indicated a clear association between Neolithic sites and areas of dark brown paleosols located within the valley bottoms (Bernabeu *et al*., 2003). This raises important questions about the origins of the dark brown paleosols that correspond to the buried A/O horizons.

In order to advance the standardization of our proposed approach, we applied REE analysis to archaeological strata in different settlements occupied since the Neolithic in the Serpis Valley (Fig. 1). More than one hundred settlements have been identified in this area (Bernabeu *et al*., 2008). Most of these open sites are characterised by dark brown strata that are very different from the typical light brown layers of the valley. The dark brown paleosol layers are usually covered by light brown paleosols and have been interpreted as markers of past anthropogenic activities (Bernabeu *et al*., 2006). Therefore, to confirm whether these strata are anthropogenic or natural, REE data and ratios values were compared with the major and minor chemical components, mineralogical properties of the soil layers and, when it was possible, cross-referenced with archaeological data to aid interpretation.

Materials and methods

A total of forty-six samples were taken through sections from six different sites, with all of the sections being c. 3 m thick. At each site, the sampling was carried out at different depths, corresponding to different layers identified by sediment colour in the field. Four sites are clearly associated with archaeological findings (sites BF, LP, PB and AC8) and another site is a place of uncertain attribution (BK5) (Bernabeu *et al*., 2006; 2008). In this section, no archaeological remains were found, but during the fieldwork, agriculture-related layers were detected (data not shown). The last site is from a natural section near the Neolithic site of Mas d'Is (MD) and has been radiocarbon dated to the first part of the Holocene (7751-7611 to 6587-6475 cal. BC) and thus predates Neolithic activity in this area (Bernabeu *et al*., 2003).

Major, minor and trace elements, including REE, were determined using X-ray fluorescence (XRF) and inductively coupled plasma-mass spectrometry (ICP-MS). Principal Components Analysis (PCA) was applied to the full set of data to identify sedimentary sources. REE ratios, Ce and Eu anomalies and La/Yb-Sm/Eu ratios were calculated for the different sites. Results were compared with the mineralogical characteristics of the layers as determined by X-ray powder diffraction (XRPD) and cross-referenced with archaeological data (MD samples were not measured by XRF and XRPD).

Soil and sediment samples

The soil samples were taken from sections at six different archaeological sites (Tab. 1 and Figs 1 and 2). With the exception of the alluvial cover, where pediments are common, most of the soil material in the study area is colluvial from the adjacent slopes, usually weathered marl that have been eroded and redeposited, covering of the marl bedrock in the Serpis Valley. Redeposited marls are easily differentiated from marls due to their discontinuity and loss of structure through the profile. Since the Islamic period, land use systems in the valley include areas of agricultural terracing, which has also contributed to the formation of colluvial soils. The maximum depth of these soils varies between two and four metres over the marl bedrock, depending on where the closest terrace is located. The dark brown layers cover, and are covered, by the colluvial soils (Diez-Castillo *et al*., 2007).

The best developed root zones are found under semi-natural vegetation. Below the root zone the soil contains a significant amount of precipitated $CaCO_3$, which is present as mottles or concretions (Diez-Castillo *et al*., 2007). For the sections sampled in this study, dark brown paleosols layers are present in AC8, PB, LP, BF and BK5. Also, as observed during the fieldwork, some of the sampled profiles are characterized by different lithologies, such as the *in-situ* Pleistocene limestone sediment in LP and PB and Miocene marl sediment in LP and BF, while more recent redeposited Miocene marls are found in PB and BK5 (Tab. 1).

The profiles were selected in order to obtain a representative set of samples belonging to natural layers with no archaeological associations and deposits associated with archaeological finds of diverse chronology, as well as a section of uncertain attribution. Latitude and longitude for these sections were determined with GPS and open data from the Spanish government (Fig. 1).

Seven samples (MD1, MD3, MD5, MD7, MD9, MD11, MD13) were taken from a Holocene natural deposit near the Mas D'Is archaeological site, characterized by light brown paleosol layers. No archaeological findings have been reported from this sampled profile (Diez-Castillo *et al*., 2011) (as mentioned above MD samples were not measured by XRF and XRPD, but just by ICP-MS). Eight samples were taken from the AC8 Planes (AC8) section, a site entirely associated with archaeological artefacts (Bernabeu *et al*., 2006) and, therefore, Holocene in age. AC81, AC82, AC83, AC84, AC85, AC86, AC87, AC88 and AC89 are from dark brown paleosol layers, however during the fieldwork it was observed that AC81, AC82, and AC89 were slightly mixed with redeposited marls. Eight samples were collected from a section at the archaeological site of Planes Benialfaquí (PB); samples PB1, PB2 were taken from an in situ red layer of Pleistocene age, while PB3, PB4 and PB5 were taken from a dark brown paleosol layer associated with early Neolithic ceramics (cardial pottery). As observed during fieldwork, the entire section is mixed with redeposited marl and this is more evident in layer PB4. PB6 was from a redeposited Miocene marl layer at the top of the section, and PB7 was collected in a redeposited Miocene marl layer that has infilled a truncation to this section (see Fig. 2). Six samples were collected

from a section at the archaeological site of La Perla (LP), located in one of the Penàguila River terraces, in the foothill of the Sierra d'Aitana; LP1 and LP2, are from the bottom of the section within a red horizon, an in situ limestone sediment of Pleistocene age. LP3 and LP4 were collected from a dark brown paleosol layer, where Neolithic sherds were found. LP5 and LP6 were both taken from a layer of redeposited Miocene marls. Nine samples were collected from a section at the archaeological site of Benifloret (BF); BF1, BF2, BF3 are from the bottom of the section and all belong to a Miocene marl layer. BF4, BF5 and BF6 were taken from a Holocene dark brown paleosol layer, where Iron Age ceramics were found (Bernabeu *et al*., 2006). BF7, BF8 and BF9 are located at the top of the section, and are redeposited sediments (Holocene light brown paleosol). Eight samples were collected in a section located between Benilloba and Benifallim at km 5 (BK5) of the road connecting these two towns, corresponding to a place of uncertain attribution, where no archaeological remains have been recorded during archaeological prospecting and fieldwork. The BK51 and BK52 samples are redeposited Miocene marls collected at the bottom of the section. BK53 and BK54 are from a dark brown paleosol layer that was subsequently buried by sediments, which then themselves under went soil formation process, producing the layers BK55 and BK56 as well as BK57 and BK58. BK55 and BK56 are from visibly more carbonate soils (interpreted during fieldwork observation as a soil developed due to recent agricultural activities) and BK57 and BK58 from an upper layer affected by contemporary agricultural activities with vegetation and roots present. However, it was difficult to define these last three layers because the boundaries between them were blurred.

Mineralogical analyses

Samples were air-dried, ground and homogenized using an agate mortar. The qualitative mineralogy of the samples was determined using a Philips PW 1830/1710 X-ray powder diffractometer (XRPD). The following experimental conditions were used: Bragg-Brentano geometry, Ni-filtered CuKα radiation obtained at 40 kV and 20 mA and 5-60° 2θ investigated range in steps of 0.02° 2θ with a step time of 2 s. The main mineralogical phases were manually identified by comparing experimental X-ray spectra with PDF2 reference patterns (DIFFRAC Plus EVA).

Major and minor elements analysis

Major and minor chemical components of the powdered samples were determined on fused glass disks using an ARL 9400 XP+ sequential X-ray spectrometer (XRF) under the instrumental conditions reported in Lezzerini *et al*. (2013). Within the range of the measured concentrations, the analytical uncertainties determined on international standards vary from 20% (Na_2O) to 1% (K_2O), with a mean value of 4% for the major and minor elements (Lezzerini *et al*., 2013; 2014). The total amount of volatile components was determined by loss on ignition (LOI) in the 105-950°C temperature range.

Trace elements and REE analysis

Sediment and soil samples were ground, homogenized by agate mortar, dried, digested and finally analyzed by ICP-MS. The soil digestion method employed is an adapted version from Guangping *et al*. (2012) and Snäll & Liljefors (2000), developed by Gallello (2014) especially for REE and other trace elements soil determination associated with clays/carbonates. The digestion method comprised addition of 1.35 ml HCl (37%) and 0.45 ml HNO_3 (69%) to 0.15 g of soil sample in borosilicate glass tubes kept at 100°C for 40 minutes in a water bath. The solutions were then carefully poured into polypropylene plastic tubes, bringing the volume to 25 ml with ultrapure water. The solutions were analyzed for: Ba, Bi, Cd, Cr, Co, Cu, Pb, Li, Mn, Mo, Ni, Sr, Tl, V, Zn and REE (La, Ce, Pr, Nd, Sm, Eu, Gd, Tb, Dy, Ho, Er, Tm, Yb, Lu), Sc and Y. A multi-element 100 µg/ml stock solution obtained from Sharlab S.L. (Barcelona) was used to prepare the calibration matrix matched standards. Concentration ranges between 1 and 600 µg/l were used for Ba, Bi, Cd, Cr, Co, Cu, Pb, Li, Mo, Ni, Sr, Tl, V, Zn, La, Ce, Pr, Nd, and concentration ranges between 1 and 100 µg/l for Sm, Eu, Gd, Tb, Dy, Ho, Er, Tm, Yb, Lu, Sc and Y. 5 ml volumetric flasks were used adding 0.15 ml of HNO_3, 0.45 ml of HCl and the corresponding volume of standard solution and were brought to volume with pure water. The digested sample solutions were filtered using Whatman number 1 filter paper and analyzed with a Perkin Elmer Elan DRCII (Concord, Ontario, Canada) ICP-MS. Soil NIM GBW07408 was used as a standard reference material for evaluating the analytical quality of the method. The standard error of the measurements during the analysis for trace elements and REE was between 1% and 3%. Rh was used as an internal standard added manually to each standard and sample solution.

Thirty-one elements were analysed and appropriate elemental mass isotopes chosen to overcome interferences. For the trace elements and REE, the analytical mass isotope instrumental detection and instrumental quantification limits (LOD and LOQ, respectively), calibration curve R^2 and ICP-MS instrument parameters are the same reported by Gallello *et al*. (2017).

REE parameters

REE concentrations in samples were normalized to Post-Archean Australian Shale (PAAS) using values

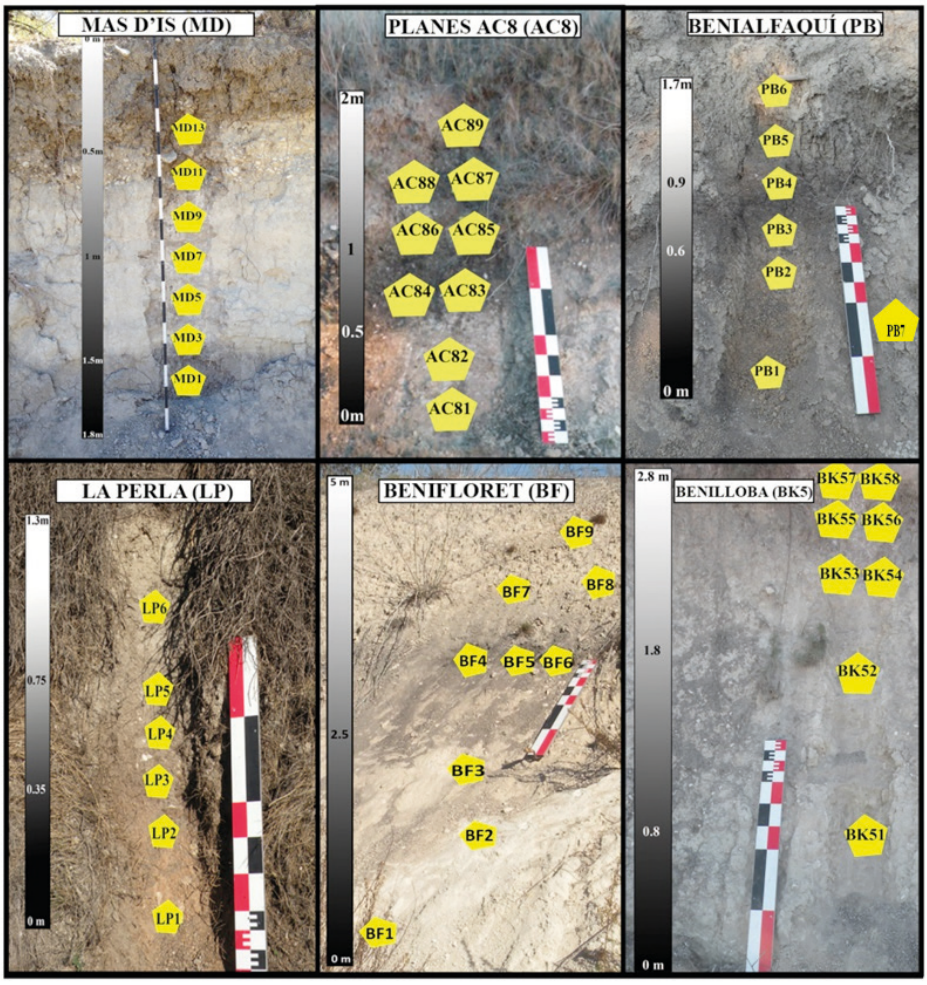

Figure 2. MD, AC8, PB, LP, BF and BK5 studied sections and sampling points.

taken from Taylor & McLennan (1985), here indicated as REE/REE_{PAAS}. This normalisation was chosen as representative of typical weathered crustal rocks. REE are commonly characterised as light (LREE: La, Ce, Pr and Nd), medium (MREE: Sm, Eu, Gd, Tb and Dy) and heavy (HREE: Ho, Er, Tm, Yb and Lu). The $REE/(REE_{PAAS})$ ratios, (where REE_{PAAS} indicate Yb, Gd and Sm values in PAAS), La/(YbPAAS), La/(GdPAAS), La/(SmPAAS) and Sm/(YbPAAS) were calculated to determine the amount of LREE, MREE, and HREE in the studied samples for each section. This method exaggerates the difference between L, M and HREE, but exaggerated differences between samples make such differences easier to be identified; we have not used the data to explore processes of geochemical fractionation. La/Yb and Sm/Eu ratios (Lisboa *et al.*, 2015) have been used in the literature to determine the provenance of sediment sources (Huang *et al.*, 2014), but they are used here to investigate differences between sections and layers.

Ce and Eu anomalies were used to determine enrichment or depletion of Ce and Eu with respect to other REE. Enrichments in Ce and Eu are indicated by an anomaly > 1 and depletion by an anomaly < 1. Cerium (4+) and Eu (2+) are the only two REE that may occur in different valance states to other REE (3+), depending on redox in typical natural environments.

The anomalies were calculated following Taylor and McLennan's equation (Taylor & McLennan, 1985), also recently used by Prajith *et al.* (2015):

$$\text{Ce anomaly} = 3(Ce/Ce_{PAAS})/(2(La/La_{PAAS}+Nd/Nd_{PAAS}))$$

$$\text{Eu anomaly} = (Eu/Eu_{PAAS})/(Sm/Sm_{PAAS} \times Gd/Gd_{PAAS})^{1/2}$$

Ce/Ce_{PAAS}, La/La_{PAAS}, Nd/Nd_{PAAS}, Eu/Eu_{PAAS}, Sm/Sm_{PAAS}, and Gd/Gd_{PAAS} represent the element concentrations normalized with respect to the same element concentration in PAAS.

Table 1. Sample description, including names of the analysed samples, location and acronyms.

Sample	Provenance	Deposit	Height* (cm)	Sample	Provenance	Deposit	Height* (cm)
MD1	Mas D'Is (MD)	Holocene light brown paleosol	0-10	**LP1**	La Perla (LP)	Pleistocene sediment	0-35
MD3	Mas D'Is (MD)	Holocene light brown paleosol	20-30	**LP2**	La Perla (LP)	Pleistocene sediment	0-35
MD5	Mas D'Is (MD)	Holocene light brown paleosol	40-50	**LP3**	La Perla (LP)	Holocene dark brown paleosol	35-75
MD7	Mas D'Is (MD))	Holocene light brown paleosol	60-70	**LP4**	La Perla (LP)	Holocene dark brown paleosol	35-75
MD9	Mas D'Is (MD)	Holocene light brown paleosol	80-90	**LP5**	La Perla (LP)	Redeposited Miocene marl sediment	75-130
MD11	Mas D'Is (MD)	Holocene light brown paleosol	100-110	**LP6**	La Perla (LP)	Redeposited Miocene marl sediment	75-130
MD13	Mas D'Is (MD)	Holocene light brown paleosol	120-130	**BF1**	Benifloret (BF)	Miocene marl sediment	80-180
AC81	Planes (AC8)	Holocene dark brown paleosol	0-54	**BF2**	Benifloret (BF)	Miocene marl sediment	80-180
AC82	Planes (AC8)	Holocene dark brown paleosol	0-54	**BF3**	Benifloret (BF)	Miocene marl sediment	80-180
AC83	Planes (AC8)	Holocene dark brown paleosol	54-110	**BF4**	Benifloret (BF))	Holocene dark brown paleosol	180-280
AC84	Planes (AC8)	Holocene dark brown paleosol	54-110	**BF5**	Benifloret (BF)	Holocene dark brown paleosol	180-280
AC85	Planes (AC8)	Holocene dark brown paleosol	110-128	**BF6**	Benifloret (BF)	Holocene dark brown paleosol	180-280
AC86	Planes (AC8)	Holocene dark brown paleosol	110-128	**BF7**	Benifloret (BF)	Holocene light brown paleosol	280-380
AC87	Planes (AC8)	Holocene dark brown paleosol	128-157	**BF8**	Benifloret (BF)	Holocene light brown paleosol	280-380
AC88	Planes (AC8)	Holocene dark brown paleosol	128-157	**BF9**	Benifloret (BF)	Holocene light brown paleosol	380-480
AC89	Planes (AC8)	Holocene dark brown paleosol	157-203	**BK51**	Benilloba (BK5)	Redeposited Miocene marl sediment	0-80
PB1	Benialfaquí (PB)	Pleistocene sediment	0-60	**BK52**	Benilloba (BK5)	Redeposited Miocene marl sediment	80-200
PB2	Benialfaquí (PB)	Pleistocene sediment	0-60	**BK53**	Benilloba (BK5)	Holocene dark brown paleosol	80-200
PB3	Benialfaquí (PB)	Holocene dark brown paleosol	60-92	**BK54**	Benilloba (BK5)	Holocene dark brown paleosol	80-200
PB4	Benialfaquí (PB)	Holocene dark brown paleosol	60-92	**BK55**	Benilloba (BK5)	Modern developed soil	200-250
PB5	Benialfaquí (PB)	Holocene dark brown paleosol	92-166	**BK56**	Benilloba (BK5)	Modern developed soil	200-250
PB6	Benialfaquí (PB)	Redeposited Miocene marl sediment	92-166	**BK57**	Benilloba (BK5)	Modern developed soil	250-280
PB7	Benialfaquí (PB)	Redeposited Miocene marl sediment	0-60	**BK58**	Benilloba (BK5)	Modern developed soil	250-280

Note: Height* indicates height from base of the sections. The dark and light brown paleosols have different characteristics (Bernabeu *et al.*, 2003; 2006; 2008; Diez-Castillo *et al.*, 2011).

Table 2. REE and trace elements values of the studied samples by ICP-MS.

SAMPLES	REE	Sc	Y	Ba	Bi	Cd	Cr	Co	Cu	Pb	Li	Mo	Ni	Sr	Tl	V	Zn
MD1	66.8	2.30	13.1	119	0.01	0.39	20.1	4.59	8.71	6.59	5.72	0.20	35.4	844	0.10	2.20	33.3
MD3	48.2	1.80	10.5	107	0.02	0.48	16.8	2.96	2.81	7.33	5.90	0.28	27.2	1053	0.07	0.05	21.1
MD5	45.4	1.68	9.92	84.6	0.01	0.62	15.0	2.76	2.37	8.11	5.39	0.28	23.9	1074	0.05	0.34	19.2
MD7	51.2	2.01	10.7	97.4	0.02	0.42	16.8	3.35	3.18	5.73	6.29	0.43	28.5	1169	0.06	1.99	19.9
MD9	54.1	2.08	11.7	88.7	0.02	0.42	18.5	3.32	3.51	5.05	6.57	0.41	28.2	1217	0.07	2.61	19.4
MD11	48.5	2.14	10.2	94.3	0.04	0.44	17.8	4.48	2.74	7.18	7.29	0.57	30.2	1312	0.06	5.81	16.0
MD13	63.7	3.13	12.0	105	0.06	1.33	22.2	5.15	7.23	42.9	10.2	0.31	33.6	969	0.10	7.51	28.4
AC81	72.0	4.64	11.8	116	0.12	0.17	24.1	7.56	7.11	9.57	18.9	0.19	35.5	454	0.09	29.0	26.1
AC82	62.8	3.30	10.8	65	0.08	0.24	21.4	5.04	0.75	6.53	22.1	0.13	28.8	780	0.05	23.9	16.5
AC83	86.2	4.56	14.0	100	0.12	0.22	27.0	7.21	8.57	10.4	22.6	0.21	35.4	544	0.10	26.0	24.5
AC84	110.3	5.91	16.4	122	0.15	0.22	33.6	8.93	11.3	12.6	29.0	0.30	41.6	517	0.12	35.0	33.9
AC85	85.9	4.69	13.6	98.2	0.11	0.23	26.8	7.07	8.17	10.4	26.7	0.20	37.5	555	0.09	29.4	26.6
AC86	99.5	5.31	15.6	113	0.13	0.23	30.3	7.77	11.8	11.4	26.9	0.26	39.5	542	0.11	31.7	30.9
AC87	85.0	4.82	14.1	95.1	0.11	0.22	27.1	7.37	6.89	9.55	28.3	0.21	37.1	611	0.10	30.3	24.7
AC88	86.7	4.92	14.3	99.3	0.12	0.20	29.2	7.21	7.69	9.92	31.2	0.20	39.5	670	0.10	35.0	23.7
AC89	77.4	4.11	12.6	102	0.11	0.21	24.3	7.70	6.31	10.5	26.1	0.23	36.9	578	0.11	28.6	19.0
PB1	96.4	5.65	14.3	145	0.15	0.18	30.8	8.62	10.1	12.0	20.0	0.70	38.3	495	0.13	36.2	28.8
PB2	88.4	5.12	13.1	126	0.13	0.18	27.3	8.07	5.75	10.9	20.0	0.50	37.0	537	0.10	32.6	23.8
PB3	119.2	6.43	18.2	149	0.03	0.19	34.7	10.6	11.4	15.6	20.8	0.29	45.7	294	0.13	22.8	38.6
PB4	80.0	4.37	13.8	130	0.04	0.30	23.7	7.67	11.8	12.9	17.0	0.12	36.7	507	0.11	37.6	33.8
PB5	140.2	7.19	20.1	158	0.04	0.22	39.9	12.2	14.2	18.4	21.6	0.23	49.4	211	0.16	27.3	52.5
PB6	66.1	3.44	12.5	119	0.02	0.14	18.3	6.59	5.59	9.42	14.8	0.10	34.4	600	0.05	13.7	16.5
PB7	52.4	2.76	9.44	63.4	0.04	0.20	17.2	4.91	3.39	6.09	17.1	0.09	29.9	718	0.04	10.0	21.7
LP1	73.3	4.25	11.8	103	0.07	0.21	24.0	7.87	4.80	9.61	15.2	0.18	32.2	362	0.10	18.4	18.9
LP2	84.7	4.59	13.4	111	0.08	0.33	26.4	8.67	4.69	10.5	17.1	0.22	34.7	352	0.10	21.1	22.4
LP3	69.4	4.21	11.2	106	0.05	0.17	24.6	7.90	4.20	9.70	14.9	0.18	36.2	485	0.08	19.1	20.6
LP4	69.8	4.22	11.3	107	0.05	0.29	24.2	7.93	3.64	10.5	15.1	0.15	36.5	478	0.08	19.5	23.3
LP5	41.7	2.49	8.17	94.2	0.03	0.17	13.6	5.60	4.14	8.13	10.2	0.11	32.1	691	0.04	14.1	13.8
LP6	39.6	2.48	7.09	109	0.07	0.14	14.9	4.97	2.68	7.17	12.0	0.17	31.0	678	0.03	24.4	12.6
BF1	43.6	2.68	7.89	97.6	0.03	0.45	22.9	4.10	3.60	9.9	10.40	0.05	30.1	853	0.05	5.45	14.6
BF2	42.4	2.69	7.71	126	0.05	0.42	14.7	4.09	2.90	9.24	9.92	0.07	30.6	823	0.05	6.91	14.7
BF3	45.8	2.64	7.45	94.4	0.05	0.22	17.0	4.09	1.73	5.78	8.53	0.10	24.8	562	0.05	9.22	12.6
BF4	62.8	3.49	10.3	132	0.04	0.30	23.1	5.74	1.58	8.3	10.3	0.09	31.5	612	0.07	10.2	18.8
BF5	67.9	3.66	10.9	151	0.05	0.53	25.2	5.91	2.76	13.6	10.3	0.13	31.8	529	0.08	12.5	22.1
BF6	81.4	4.60	12.8	146	0.05	0.27	30.2	6.98	6.29	10.45	12.0	0.14	39.2	435	0.11	14.2	28.3
BF7	54.3	2.70	8.80	89.9	0.03	0.25	18.3	4.27	3.57	7.65	8.70	0.08	25.3	627	0.06	6.58	14.8
BF8	56.8	2.79	9.31	100	0.03	0.29	18.3	4.60	2.87	7.80	8.37	0.10	27.0	606	0.06	4.25	14.7
BF9	53.3	2.44	8.46	90.2	0.03	0.54	16.8	4.09	2.82	12.74	7.8	0.08	24.1	651	0.07	4.57	16.0
BK51	51.5	2.90	9.37	106	0.04	0.34	16.7	4.92	3.46	11.3	18.5	0.11	28.3	784	0.04	12.2	21.3
BK52	46.1	2.39	8.63	124	0.02	0.17	13.8	4.76	2.72	7.16	15.1	0.09	26.4	722	0.03	7.75	18.1
BK53	56.6	3.17	9.87	136	0.02	0.18	19.9	6.01	4.75	8.25	16.1	0.10	30.7	591	0.06	12.0	19.7
BK54	55.8	3.14	10.3	127	0.02	0.19	19.4	5.26	3.42	7.82	16.1	0.10	29.0	603	0.04	10.9	18.8
BK55	64.7	3.65	11.4	145	0.01	0.19	22.9	7.12	4.72	8.93	18.0	0.11	34.7	543	0.07	11.9	24.7
BK56	56.5	3.02	10.4	123	0.00	0.19	18.2	5.83	3.83	8.10	14.3	0.08	30.6	517	0.05	9.36	16.2
BK57	77.5	4.32	13.3	164	0.02	0.20	27.1	7.45	7.47	10.5	20.2	0.13	37.3	565	0.08	16.6	29.8
BK58	72.4	3.78	14.0	170	0.02	0.20	22.3	7.16	5.60	10.2	17.4	0.09	36.3	596	0.06	11.1	25.2

Concentration of elements in μg/g. REE indicates the total sum of REE.

Table 3. Major and minor chemical components of the studied samples determined by XRF.

SAMPLE	L.O.I.	Na_2O	MgO	$A_{l2}O3$	SiO_2	P_2O_5	K_2O	CaO	TiO_2	MnO	Fe_2O_3 T
AC81	30.9	0.07	1.20	4.47	20.5	0.18	1.08	37.87	0.30	0.04	3.42
AC82	30.5	0.08	1.26	4.66	21.2	0.18	1.13	36.93	0.33	0.04	3.70
AC83	26.8	0.10	1.54	6.76	27.5	0.23	1.64	29.70	0.47	0.06	5.27
AC84	23.8	0.11	1.77	8.19	32.1	0.24	1.88	25.13	0.58	0.07	6.15
AC85	28.4	0.09	1.48	6.07	24.9	0.23	1.49	32.08	0.42	0.05	4.79
AC86	25.5	0.10	1.64	7.33	29.2	0.26	1.74	27.94	0.52	0.07	5.73
AC87	28.2	0.09	1.50	6.38	25.7	0.23	1.56	30.81	0.43	0.05	5.04
AC88	29.4	0.08	1.41	5.69	23.3	0.22	1.42	33.43	0.39	0.05	4.59
AC89	28.0	0.09	1.52	6.34	26.0	0.20	1.53	30.85	0.44	0.05	4.99
PB1	23.9	0.13	1.66	7.96	31.2	0.11	1.85	26.70	0.57	0.07	5.90
PB2	25.9	0.10	1.44	6.86	27.5	0.13	1.65	30.29	0.51	0.05	5.59
PB3	18.5	0.13	2.23	11.2	40.8	0.14	2.18	17.04	0.77	0.08	6.96
PB4	15.3	0.12	2.23	11.8	44.2	0.12	2.43	14.74	0.89	0.09	8.04
PB5	28.3	0.10	1.57	6.71	27.5	0.14	1.44	28.73	0.48	0.05	4.95
PB6	28.8	0.10	1.50	5.93	25.3	0.16	1.29	32.05	0.41	0.04	4.40
PB7	26.6	0.10	1.46	6.95	27.3	0.20	1.63	30.08	0.49	0.06	5.14
LP1	25.8	0.10	1.37	7.64	27.8	0.12	1.75	29.18	0.54	0.04	5.68
LP2	24.5	0.11	1.48	8.30	30.0	0.13	1.87	26.91	0.60	0.05	6.05
LP3	25.2	0.11	1.55	8.41	30.2	0.12	1.80	25.92	0.60	0.06	6.11
LP4	27.9	0.10	1.37	7.21	26.1	0.13	1.59	29.69	0.52	0.05	5.35
LP5	35.1	0.08	1.01	4.47	17.0	0.15	1.12	37.45	0.31	0.03	3.34
LP6	36.2	0.07	0.94	3.98	15.4	0.16	1.05	39.00	0.27	0.03	2.92
BF1	31.3	0.09	1.51	4.57	21.1	0.17	1.18	36.10	0.29	0.05	3.61
BF2	32.3	0.08	1.44	4.48	19.6	0.18	1.21	36.98	0.29	0.04	3.49
BF3	31.5	0.07	1.45	4.68	20.3	0.16	1.19	36.70	0.33	0.04	3.60
BF4	25.5	0.13	1.93	7.68	30.4	0.16	1.71	26.15	0.55	0.07	5.75
BF5	28.7	0.09	1.67	6.13	25.1	0.15	1.40	31.73	0.43	0.04	4.64
BF6	29.9	0.08	1.66	5.69	23.3	0.15	1.35	33.09	0.39	0.04	4.35
BF7	31.0	0.08	1.66	4.84	21.7	0.17	1.22	35.40	0.33	0.04	3.56
BF8	30.6	0.08	1.53	5.05	22.0	0.16	1.26	35.04	0.35	0.04	3.81
BF9	31.3	0.08	1.65	4.71	21.0	0.16	1.18	36.06	0.32	0.03	3.47
BK51	29.9	0.12	2.05	4.55	24.0	0.17	1.19	34.15	0.31	0.04	3.55
BK52	31.1	0.10	1.84	4.26	21.4	0.17	1.15	36.19	0.30	0.04	3.41
BK53	29.1	0.12	2.00	5.21	24.3	0.15	1.32	33.23	0.37	0.05	4.15
BK54	29.0	0.13	2.01	5.26	24.4	0.16	1.32	33.10	0.37	0.05	4.19
BK55	26.8	0.12	2.14	6.28	28.1	0.17	1.56	29.13	0.48	0.06	5.18
BK56	27.4	0.11	1.97	5.87	26.4	0.16	1.54	30.85	0.47	0.06	5.18
BK57	26.7	0.12	2.13	6.30	28.7	0.18	1.56	28.57	0.50	0.07	5.23
BK58	25.3	0.12	2.13	6.49	30.2	0.18	1.64	27.65	0.54	0.08	5.69

Concentration of elements are expressed as weight percentage (wt%).

Data analysis

Statistical analysis was carried out on the full sample set. The REE, Sc and Y were used as variables for Principal Component Analysis (PCA) modeling. PCA was used to explore the large geochemical datasets, reducing the number of variables and providing a deep insight into the structure of the variance of the dataset. For PCA, 39 samples and 16 variables (La/La_{PAAS}, Ce/Ce_{PAAS}, Pr/Pr_{PAAS}, Nd/Nd_{PAAS}, Sm/Sm_{PAAS}, Eu/Eu_{PAAS}, Gd/Gd_{PAAS}, Tb/Tb_{PAAS}, Dy/Dy_{PAAS}, Ho/Ho_{PAAS}, Er/Er_{PAAS}, Tm/Tm_{PAAS}, Yb/Yb_{PAAS}, Lu/Lu_{PAAS}, Sc/Sc_{PAAS}, Y/Y_{PAAS}) have been employed to run the analysis. Mean centering and autoscaling pre-processing prior to modeling were used, cross validation (CV) was carried out employing venetian blinds with 6 splits and 1 sample per split (Jolliffe, 2002; Wise *et al*., 2006).
Data analysis was carried out using the PLS Toolbox 8.2 for Eigenvector Research Inc., (Wenatchee, WA, USA) running in Matlab R2016b from Mathworks Inc., (Natick, MA, USA).

Results and discussion

Serpis Valley sediments geochemical data

Results of total REE, trace elements and major elements are reported in Tabs 3 and 4; individual REE concentrations, absolute and PAAS normalized REE, Sc and Y are provided in Supplementary Materials (Annex I and Annex II). The data shows that the excavated sections have different geochemical compositions. The total REE, Sc and Y (Tab. 2) in general had higher concentrations in archaeological layers, while the lower values occurred in natural deposits; by comparison major and minor elements did not clearly show differences between non-anthopogenic and archaeological layers in the studied profiles (Tab. 2).
Looking at correlations, in the natural profile MD, total REE (except Sc and Y) are highly correlated with Cu, Ni, Cr and Zn (R^2 0.80-0.90; $p < 0.01$), and negatively correlated with Sr (R^2 0.50, $p < 0.0003$). For the archaeological profile AC8, total REE correlate strongly with Cr, Cu, Ni and Zn (R^2 0.76-0.95; $p < 0.01$), and less strongly with Ba and V (R^2 0.50-0.57; $p < 0.01$). Positive correlations between the total REE and Na_2O, MgO, Al_2O_3, SiO_2, P_2O_5, K_2O, TiO_2, MnO and Fe_2O_3T (R^2 0.67-0.85; $p < 0.01$) and a negative correlation with LOI and CaO (R^2 0.83-0.81; $p < 0.01$) are also evident. In the PB profile, total REE correlate strongly with Ba, Cr and Zn (R^2 0.73-0.97; $p < 0.01$) and negatively with Sr (R^2 0.97; $p< 0.01$), but no correlations with major elements and LOI were found. In the LP profile, total REE correlate strongly with Cr (R^2 0.95; $p < 0.01$) and Zn (R^2 0.84; $p < 0.01$), and there is a strong negative correlation between total REE and Sr (R^2 0.94; $p < 0.01$). Between LOI and major elements, Na_2O, MgO, Al_2O_3, SiO_2, K_2O, TiO_2, MnO and Fe_2O_{3T} positively correlate with total REE in this profile (R^2 0.60-0.94; $p < 0.01$), while P_2O_5, and CaO (R^2 0.74-0.88; $p< 0.01$) and LOI (R^2 0.94; $p < 0.01$) have a negative correlation. In the BF profile, total REE are correlated with Cr (R^2 0.68 $p < 0.01$) and Zn (R^2 0.87 $p < 0.01$), while V correlates with total REE less strongly (R^2 0.55; $p< 0.01$), and Sr has a negative correlation (R^2 0.67; $p< 0.01$). For the major elements no correlation with total REE was found in the BF profile. Finally, in BK5 total REE strongly correlate with Ba, Cr, and Zn (R^2 0.75-0.93; $p < 0.01$), and have a weaker correlation with V (R^2 0.54; $p < 0.01$). A positive correlation between total REE and MgO, Al_2O_3, SiO_2, K_2O, TiO_2, MnO and Fe_2O_{3T} (R^2 0.70-0.85; $p < 0.01$) was observed, and there is a strong negative correlation with LOI (R^2 0.79; $p < 0.01$) and CaO (R^2 0.86; $p < 0.01$).
In Tab. 4, the qualitative mineralogy of the samples is shown. Calcite is equally abundant for every sample except for PB2, PB3, PB4 that contain lower amounts. Dolomite was identified in BK51, BK54, BK56 and traces of this mineral were found in BF1, BF3, BF4, BF5, BF7, BF8, BK52, BK53, BK55, BK58, LP6, PB1, AC83 and AC85. Quartz was found in all the samples, but it is especially abundant in samples PB3 and PB4. Finally, traces of feldspars and phyllosilicates were found in almost all the samples; LP1 contained more feldspars than the other samples. As with the major and minor elements, the mineralogical phases in the studied sections did not clearly indicate differences between the natural and anthropogenic deposits. However, in profile AC8, the bottom samples AC81 and AC82 are the only ones with traces of phyllosilicates and this corresponds with the lowest REE concentrations in this profile. Profile LP has lower amounts of quartz in samples LP5 and LP6, and their REE concentrations are the lowest. In BF, the opposite situation to that in AC8 is observed: the absence of phyllosilicates in samples BF7 and BF8 coincides with lower concentrations of total REE. For BK5, the absence of feldspars in samples BK57 and BK58 coincides with the highest total REE levels throughout the profile.

REE distribution in the Serpis Valley

Correlations between La/Yb and Sm/Eu ratios (Fig. 3) were used in an attempt to identify differences between the studied sections. The high correlation (R^2 0.80; $p = <0.0001$) could suggest that there are different weathering processes that occurred during layer formation, especially taking into account the differences between Holocene dark brown and light brown paleosols – the first with relatively high La/Yb and Sm/Eu ratios, and the second with relatively low values of ratios. However, on the basis of the available data, distinct source materials or lithologies are con-

Table 4. Mineralogy of studied samples as determined by XRPD.

SAMPLE	Calcite	Dolomite	Quartz	Feldspars	Phyllosilicates
AC81	XXX	-	XX	tr	tr
AC82	XXX	-	XX	tr	tr
AC83	XXX	tr	XX	tr	-
AC84	XXX	-	XX	tr	-
AC85	XXX	tr	XX	tr	-
AC86	XXX	-	XX	tr	-
AC87	XXX	-	XX	tr	-
AC88	XXX	-	XX	tr	-
AC89	XXX	-	XX	tr	tr
PB1	XXX	tr	XX	tr	tr
PB2	XX	-	XX	tr	tr
PB3	XX	-	XXX	tr	tr
PB4	XX	-	XXX	tr	tr
PB5	XXX	-	XX	tr	tr
PB6	XXX	-	XX	tr	tr
PB7	XXX	-	XX	tr	tr
LP1	XXX	-	XX	X	tr
LP2	XXX	-	XX	tr	tr
LP3	XXX	-	XX	tr	tr
LP4	XXX	-	XX	-	-
LP5	XXX	-	X	tr	tr
LP6	XXX	tr	X	tr	tr
BF1	XXX	tr	X	tr	tr
BF2	XXX	-	X	-	tr
BF3	XXX	tr	XX	tr	tr
BF4	XXX	-	XX	tr	tr
BF5	XXX	tr	XX	tr	tr
BF6	XXX	tr	XX	tr	tr
BF7	XXX	tr	XX	tr	-
BF8	XXX	tr	XX	tr	-
BF9	XXX	-	XX	tr	tr
BK51	XXX	X	X	tr	tr
BK52	XXX	tr	X	tr	tr
BK53	XXX	tr	X	tr	tr
BK54	XXX	X	X	tr	tr
BK55	XXX	tr	XX	tr	tr
BK56	XXX	X	X	tr	tr
BK57	XXX	-	X	-	tr
BK58	XXX	tr	XX	-	tr

Note: semi-quantitative values. Highly abundant (XXX), abundant (XX), present (X), trace (tr). No detected (-).

tributing to the formation of the studied sections and are susceptible to REE changes sometime in a similar way between them, consequently Pleistocene sediment samples are comparable to Holocene dark brown paleosols, and Miocene marl sediment and redeposited marl comparable to the Holocene light brown paleosols in their La/Yb and Sm/Eu ratio values.

Principal Component Analysis (PCA) was applied to all samples using the fourteen REE/REE_{PAAS} plus Sc/Sc_{PAAS} and Y/Y_{PAAS} (Figs 4a and 4b) as variables; the score plots were represented as data points (samples) projected into the PC space. In view of the La/Yb and Sm/Eu ratios results (Fig. 3) the layers belonging to different lithologies such as the Miocene marl sediments and Pleistocene sediments were not included in PCA modelling, which just considered deposits formed during the Holocene period.

PCA in Fig. 4a shows the distribution of samples in different groups. The first two principal components explain 99.12% in the variance of data: PC1 93.33% and PC2 5.79%, respectively. Magnitude and signs of the loadings on the Y axis (Fig. 4b) show that La/La_{PAAS}, Ce/Ce_{PAAS}, Pr/Pr_{PAAS}, Nd/Nd_{PAAS}, Sm/Sm_{PAAS}, Eu/Eu_{PAAS}, Gd/Gd_{PAAS}, Tb/Tb_{PAAS}, Dy/Dy_{PAAS}, Ho/Ho_{PAAS}, Er/Er_{PAAS}, Tm/Tm_{PAAS}, Yb/Yb_{PAAS}, Lu/Lu_{PAAS}, Sc/Sc_{PAAS} and Y/Y_{PAAS} are all important variables for PC1 and La/La_{PAAS}, Ce/Ce_{PAAS}, Pr/Pr_{PAAS}, Nd/Nd_{PAAS}, Sm/Sm_{PAAS}, Ho/Ho_{PAAS}, Er/Er_{PAAS}, Tm/Tm_{PAAS}, Yb/Yb_{PAAS}, Lu/Lu_{PAAS} and Sc/Sc_{PAAS} are the most important for PC2 to obtain the plot distribution. The fact that in PC1 all the REE have a similar loading suggests that they are behaving as a coherent group and their variation in concentrations are going up and down in proportion to each other. By contrast PC2 represents variation between individual REE. The LREE show an inverse relationship with the HREE and so correlated with La/Yb ratio sample distribution (Fig. 3).

PCA shows differences in the excavated sections based on the layers characteristics. The majority of the samples from Holocene brown dark soils plot together in the right part of the plot. On the left of the PC, Holocene light brown soils are grouped together with redeposited Miocene marl samples (Fig.1). All the MD samples, taken from the Holocene light brown paleosol, plot at the top of the figure in the middle of the x axis. Within the modern developed soil, samples BK55 and BK56 are plotted on the centre left side of the PC, while BK57 and BK58 are on the centre right side; all of them close to the Holocene dark brown paleosols. Finally, BK53 and BK54 classified as Holocene dark brown paleosols are plotted on the left side, but still separated from the redeposited Miocene marl, while the redeposited Miocene marl PB6 is grouped closer to the Holocene dark brown paleosols BF4 and BF5. The PCA results show a quite clear difference between dark brown (anthropogenic) paleosols and light brown (natural) paleosols.

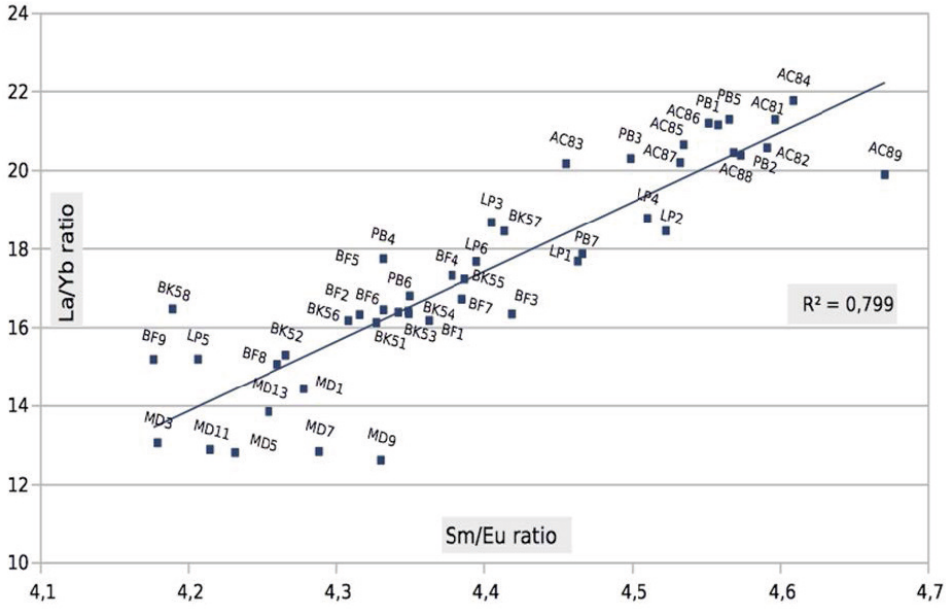

Figure 3. La/Yb-Sm/Eu correlation of the full set of samples. R^2 coefficient and *p* value are shown.

REE ratios, Ce and Eu anomalies

Differences between archaeological and natural layers can be also observed by examining the Holocene developed layers employing REE ratios, La/(Yb_{PAAS}), La/(Gd_{PAAS}), La/(Sm_{PAAS}) and Sm/(Yb_{PAAS}), and Ce and Eu anomalies (Tab. 5).

MD is not associated with archaeological remains (Diez-Castillo *et al.*, 2011). Higher REE/(REE_{PAAS}) values in MD1 and MD13 were not related to the stratigraphic position. Ce and Eu negative anomalies (<1) were present throughout the section and the anomaly values for MD1 and MD13 were very similar. AC8 is a deep section, entirely related to archaeological remains where Neolithic ceramics were found (Bernabeu *et al.*, 2008). The top sample AC89 was distinct from the AC83-AC88 middle section samples, with AC84 and AC86 having larger REE/(REE_{PAAS}) values and less negative Eu anomalies compared to the other middle section samples. PB is a section located at around 1 kilometre from AC8; Neolithic ceramics were found in this section associate with the layers where samples PB3 and PB5 were collected (Bernabeu *et al.*, 2008). This section is also characterized by the disturbance of redeposited Miocene marls. PB3 and PB5 (brown dark soils related to archaeological finds) show negative Ce and Eu anomalies, have higher REE/(REE_{PAAS}) values and smaller Eu anomalies, and are clearly grouped separately from the other samples. The LP section is located in the foothill of the Sierra d'Aitana and consists of Neolithic period dark brown soils. REE/(REE_{PAAS}) ratios and negative Eu anomalies show LP3 and LP4 values higher than the redeposited marl samples (LP5 and LP6). BF is a section located 6 km from LP and BK5 with archaeological remains including Iron Age ceramics found in dark brown paleosol layers. REE/(REE_{PAAS}) and negative Eu anomalies show differences between the natural deposits at the top (BF1-BF3) of the section and the dark brown paleosol samples (BF4-BF6). BF4-BF6 show high REE ratios values and a less negative Eu anomaly. BK5, located close to the LP excavation, is a place where no archaeological finds have been documented. These samples comprise a dark brown paleosol layer (BK53-BK54) and a developed soil layer (BK55-BK56 probably formed by recent agricultural activities), which occur in the middle of the section. REE/(REE_{PAAS}) ratios and negative Eu anomalies show BK53-BK56 values are between the low value of the redeposited marl samples and the high values of the contemporary agricultural developed soil samples (BK57-BK58).

REE distribution processes in the profiles

As described in the previous section, the REE profiles of layers associated with archaeological evidence were generally characterized by higher REE levels and weaker negative Eu anomalies. In contrast, those layers identified during fieldwork as being unrelated to archaeological findings (corresponding to light brown paleosols and redeposited marls) have lower REE values and more negative Eu anomalies. Mineralogy, major and minor compounds were not able to detect differences between the layers (Tab. 1, Tab. 2 and Tab. 3). Similarly, REE correlations with major and minor elements did not indicate any clear difference between layers that permit differentiation between those that were anthropogenic or natural.

In general, the mechanisms that control the REE behaviour are associated with the sedimentary environ-

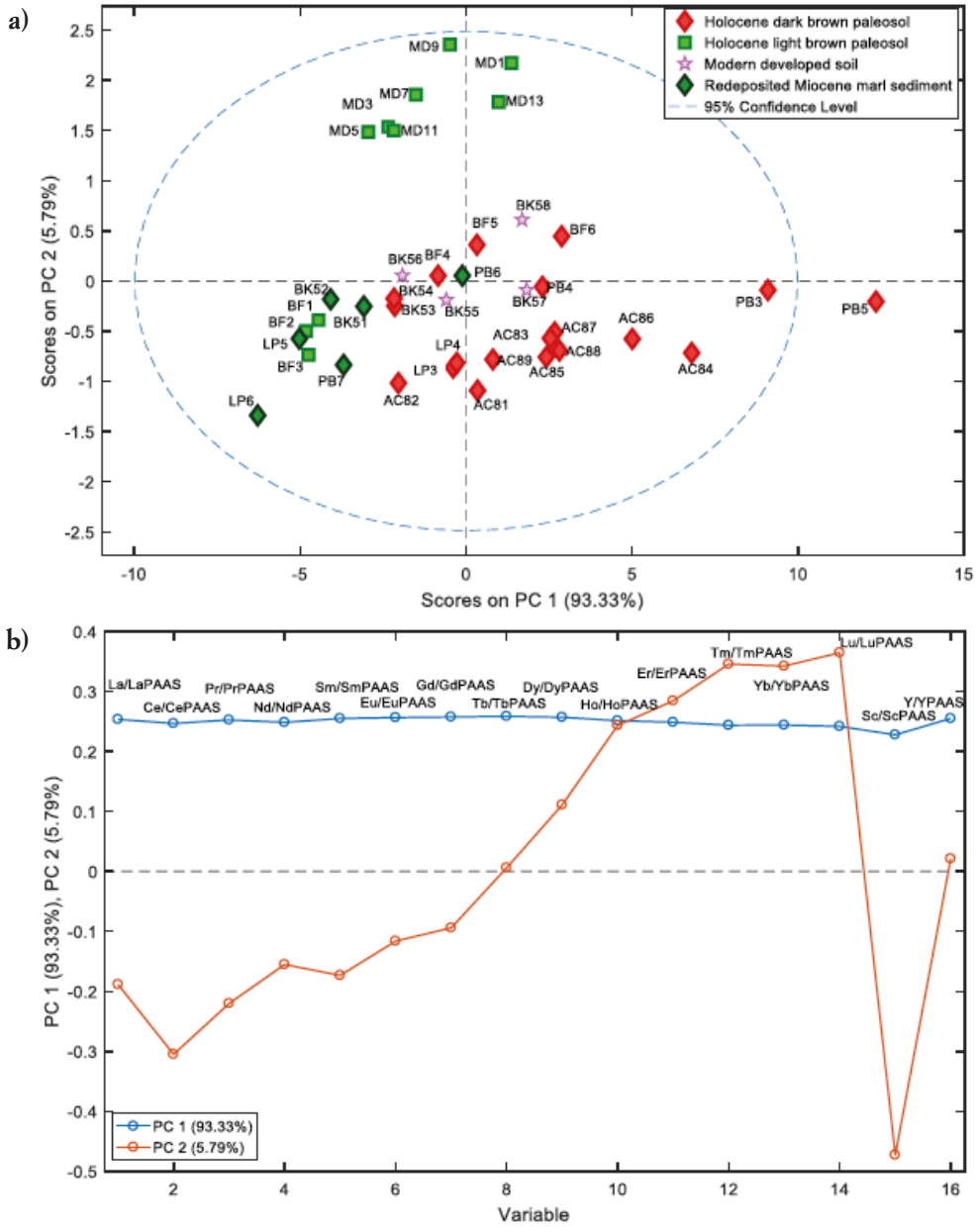

Figure 4. PCA of the studied soil samples employing REE. Scores (a) and loadings of 0. Y axis (b) plot of PC1 and PC2. Factor loadings above 0.1 or more negative than -0.1 were considered as high, and were used for the interpretation of the principal components.

ment. In the Serpis Valley, the bedrock is marl, a calcium carbonate-rich mudrock. Except where there is a direct or indirect anthropogenic contribution, soils are formed by the weathering of this bedrock, including the development of dark brown paleosols rich in carbonate (Gallello *et al.*, 2013), which could potentially exert an important influence on their REE distributions (Laveuf & Cornu, 2009). The mineralogy of the whole set of samples is characterized by abundant amounts of calcite and the almost complete absence of dolomite suggesting that pedogenic carbonate also plays an important role in REE distribution throughout the profiles, as reported elsewhere by West *et al.* (1988).

Complexation and leaching of REE with carbonate ions has been reported by some authors (Taylor & McLennan, 1979; Michard *et al.*, 1987; Lee & Byrne 1993; Koppi *et al.*, 1996; Land *et al.*, 1999; Hu *et al.*, 2006; Laveuf & Cornu, 2009). Negative Ce and Eu anomalies can be generated by the presence of calcareous and siliceous organisms in carbonate environments, as may also be occurring in our case study. Furthermore, weathered products and secondary minerals including phillipsites, phosphorites and smectites (Pattan *et al.*, 2005) can contribute in the development of the strong REE migration occurring during the weathering process of carbonate rocks (Jiyan & Ruidong, 2010).

Table 5. Cerium and Europium anomalies values and REE ratios of the studied samples belonging to Holocene brown and light paleosols, redeposited Miocene sediments, and modern developed soils.

Sample	Provenance	Ce Anomaly	Eu Anomaly	La/(YbPAAS)	La/(GdPAAS)	La/(SmPAAS)	Sm/(YbPAAS)
MD1	Holocene light brown paleosol	0.72	0.59	4.92	2.45	2.15	0.97
MD3	Holocene light brown paleosol	0.67	0.52	3.57	1.78	1.56	0.72
MD5	Holocene light brown paleosol	0.67	0.50	3.35	1.67	1.47	0.68
MD7	Holocene light brown paleosol	0.67	0.52	3.78	1.88	1.65	0.77
MD9	Holocene light brown paleosol	0.66	0.53	4.02	2.00	1.76	0.82
MD11	Holocene light brown paleosol	0.67	0.52	3.58	1.79	1.57	0.73
MD13	Holocene light brown paleosol	0.73	0.59	4.53	2.26	1.98	0.95
AC81	Holocene dark brown paleosol	1.03	0.60	5.63	2.80	2.46	1.09
AC82	Holocene dark brown paleosol	0.79	0.53	4.56	2.27	1.99	0.87
AC83	Holocene dark brown paleosol	0.83	0.64	6.08	3.03	2.66	1.18
AC84	Holocene dark brown paleosol	0.84	0.70	7.77	3.87	3.40	1.51
AC85	Holocene dark brown paleosol	0.83	0.63	6.06	3.02	2.65	1.19
AC86	Holocene dark brown paleosol	0.81	0.67	7.17	3.57	3.14	1.36
AC87	Holocene dark brown paleosol	0.81	0.62	6.12	3.05	2.68	1.15
AC88	Holocene dark brown paleosol	0.81	0.62	6.22	3.10	2.72	1.20
AC89	Holocene dark brown paleosol	0.83	0.58	5.50	2.74	2.41	1.07
PB3	Holocene dark brown paleosol	0.85	0.75	8.26	4.12	3.61	1.64
PB4	Holocene dark brown paleosol	0.81	0.64	5.57	2.78	2.44	1.14
PB5	Holocene dark brown paleosol	0.88	0.79	9.67	4.82	4.23	1.90
PB6	Redeposited Miocene marl sediment	0.77	0.59	4.67	2.33	2.05	0.97
PB7	Redeposited Miocene marl sediment	0.81	0.50	3.65	1.82	1.60	0.74
LP3	Holocene dark brown paleosol	0.85	0.58	4.76	2.37	2.08	0.97
LP4	Holocene dark brown paleosol	0.85	0.57	4.77	2.38	2.09	0.98
LP5	Redeposited Miocene marl sediment	0.77	0.49	2.89	1.44	1.26	0.63
LP6	Redeposited Miocene marl sediment	0.79	0.45	2.80	1.40	1.23	0.58
BF4	Holocene dark brown paleosol	0.80	0.64	5.75	2.87	2.52	1.14
BF5	Holocene dark brown paleosol	0.79	0.59	4.76	2.37	2.08	0.98
BF6	Holocene dark brown paleosol	0.80	0.57	4.40	2.19	1.93	0.91
BF7	Holocene light brown paleosol	0.78	0.48	3.23	1.61	1.42	0.66
BF8	Holocene light brown paleosol	0.75	0.49	2.98	1.49	1.30	0.64
BF9	Holocene light brown paleosol	0.74	0.51	3.06	1.52	1.34	0.67
BK51	Redeposited Miocene marl sediment	0.76	0.52	3.64	1.81	1.59	0.76
BK52	Redeposited Miocene marl sediment	0.75	0.51	3.24	1.62	1.42	0.69
BK53	Holocene dark brown paleosol	0.78	0.55	3.97	1.98	1.74	0.83
BK54	Holocene dark brown paleosol	0.77	0.54	3.93	1.96	1.72	0.82
BK55	Modern developed soil	0.79	0.58	4.53	2.26	1.98	0.94
BK56	Modern developed soil	0.77	0.55	3.98	1.99	1.74	0.83
BK57	Modern developed soil	0.80	0.62	5.50	2.74	2.41	1.11
BK58	Modern developed soil	0.77	0.64	5.08	2.53	2.22	1.06

The changes of REE occurring in this sedimentary environment based in carbonate rocks could account for the high La/Yb and Sm/Eu correlation. However, it is possible that differences in these correlations may result from sediments deriving from different lithologies.
Organic compounds can have distinct REE signatures (Laveuf & Cornu, 2009). In this study, we did not separate out and analyse organic matter from the sediments and, therefore, we cannot determine whether the higher REE values in the archaeological deposits are due to the presence of some organic compounds. However, human activities such as agriculture can lead to the enrichment of soil organic matter, which can be retained during paleosol formation (Hu *et al*., 2006). REE can migrate between layers and could be retained in the soil formed during human occupation by complexation with immobile organic compounds (Hu *et al*., 2006). This would result in higher REE concentrations in anthropogenic layers compared with natural layers.
Section BK5 comprises redeposited marl, Holocene dark brown paleosols that contain no archaeological remains, and recently developed agricultural soils. Such a section allows us to test the efficacy of REE ratios to discriminate between layers of different origin. REE/(REE_{PAAS}) and Eu anomalies show differences between the redeposited marls (BK51 and BK52) and the other layers. The Holocene dark brown paleosols (BK53 and BK54) and recent agricultural soil layer (BK55 and BK56) show similar values. However, the contemporary agricultural soils (BK57 and BK58) are different from Holocene dark brown paleosol and recent agricultural soil layer with higher REE values probably due to the presence of roots and vegetation (Hu *et al*., 2006). All this suggests the potential of REE to discriminate the Holocene dark brown layers as anthropogenic compared to Holocene light brown as natural.

Conclusions

The use of REE analysis of anthropogenic layers helps to confirm differences between natural and human activities in this case study. Changes between layers are especially highlighted by REE/(REE_{PAAS}) and Eu anomalies; archaeological layers show different concentrations of REE than the natural deposits. However, at the moment, it is not possible to confirm if this is due to the presence of organic matter or whether there are other soil compounds influencing the REE levels in the archaeological layers.
Importantly, we confirmed that correlations between La/Yb and Sm/Eu could be used to confirm the presence of material from different sources and/or origins (natural vs anthropogenic) in soils and sediments sampled from the same section. This provides a foundation for the development of future tests to standardize the use of these ratios in soil sections in different environments worldwide.
Although the potential of REE to link strata with no reported archaeological finds to anthropogenic activities is supported by our findings of similar REE patterns in the dark brown paleosols and recent soil of an agricultural origin, more specific studies involving organic compounds analyses need to be carried out in this region to fully prove or disprove this finding. We have shown that REE can help to confirm the archaeological interpretation, pointing out that these dark brown deposits are evidence of past human activities in the Serpis Valley.
Finally, more soil and sediment features need to be analysed from more excavated sections, as well as from a range of sedimentary environments (e.g. ongoing work in basalt sediments) need to be studied to standardize the use of REE as tracers of anthropogenic and natural deposits.

Acknowledgements

The authors acknowledge the financial support of the European Commission (Projects H2020-MSCA-IF-2015-704709-MATRIX and ERC-StG-2012-337128-AAREA).
Agustin Pastor acknowledges the financial support of Generalitat Valenciana (PROMETEO project II/2014/077) and Ministerio de Economia y Competitividad-Feder (Project CTQ 2014-52841-P and Project CTQ 2012-38635).

References

Bernabeu J., Orozco T., Díez A., Gómez M., Molina J.F., 2003. Mas d'Is (Penàguila, Alicante): aldeas y recintos monumentales del Neolítico inicial en el Valle del Serpis. *Trabajos de Prehistoria* 60: 39-60.

Bernabeu J., Molina L.L., Díez Castillo A., Orozco Köhler T., 2006. Inequalities and power. Three millennia of Prehistory in Mediterranean Spain (5600-2000 cal BC). In Diaz-del-Río y, P., García Sanjuán, L. (Eds.). Social Inequality in Iberian Late Prehistory. *British Archaeological Reports*, *International Series* 1525: 97-116.

Bernabeu J., Molina L.L., Orozco T., Diez A., Barton C.M., 2008. Early Neolithic at the Serpis Valley, Alicante, Spain. In Diniz, M. ed. *The Early Neolithic in the Iberian Peninsula*, Bar IS-1587.

Cook D.E., Kovacevich B., Beach T., Bishop R., 2006. Deciphering the inorganic chemical record of ancient human activity using ICP-MS: a reconnaissance study of Classic soil floors at Cancuén, Guatemala. *Journal of Archaeological Science* 33: 628-640.

Diez-Castillo A., Barton C.M., La Roca Cervigón N., Bernabeu J., 2007. *Landscape Socioecology in the Serpis Valley* (10,000-4000 BP). In Layers of Perception – CAA 2007, 2007.

DIEZ-CASTILLO A., BERNABEU AUBAN J., OROZCO KÖHLER T., LA ROCA CERVIGÓN N., 2011. Las campañas de excavación de 2010 y 2011 en el yacimiento neolítico del Mas d'Is (Penàguila, Alacant). *SAGVNTVM, Papeles del Laboratorio de Arqueología de Valencia* 42: 105-109.

GALLELLO G., PASTOR A., DIEZ A., LA ROCA N., BERNABEU J., 2013. Anthropogenic units fingerprinted by REE in archaeological stratigraphy: Mas d'Is (Spain) case. *Journal of Archaeological Science* 40: 799-809.

GALLELLO G., 2014. Western Mediterranean Archaeology: chemical element levels in archaeological materials as a methodological tool. Dissertation. Universitat de València. *ProQuest* editor, ISBN: 978-1-303-99720-4, 245 pp.

GALLELLO G., PASTOR A., DIEZ A., BERNABEU J., 2014. Lanthanides revealing anthropogenic impact within a stratigraphic sequence. *Journal of Archaeology* http://dx.doi.org/10.1155/2014/767085.

GALLELLO G., RAMACCIOTTI M., LEZZERINI M., HERNANDEZ E., CALVO M., MORALES A., PASTOR A., DE LA GUARDIA M., 2017. Indirect chronology method employing rare earth elements to identify Sagunto Castle mortar construction periods. *Microchemical Journal* 132: 251-261.

GUANGPING X., HANNAH J.L., BINGEN B., GEORGIEV S., STEIN H.J., 2012. Digestion methods for trace element measurements in shales: Paleoredox proxies examined. *Chemical Geology* 324-325: 132-147.

HU Z., HANEKLAUS S., SPAROVEK G., SCHNUG E., 2006. Rare earth elements in soils. *Communications in soil science and plant analysis* 37: 1381-1420.

HUANG H., DU Y., YANG J., ZHOU L., HU L., HUANG H., HUANG Z., 2014. Origin of Permian basalts and clastic rocks in Napo, Southwest China: Implications for the erosion and eruption of the Emeishan large igneous province. *Lithos* 208-209: 324-338.

JIYAN C., RUIDONG Y., 2010. Analysis on REE geochemical characteristics of three types of REE-rich soil in Guizhou Province, China. *Journal of Rare Earths*, 28: 517-522.

JOLLIFFE I.T., 2002. Principal Component Analysis. second ed. *Springer-Verlag*, New York. DOI: 10.1007/b98835.

KAMENOV G.D., BRENNER M., TUCKER J.L., 2009. Anthropogenic versus natural control on trace element and Sr-Nd-Pb isotope stratigraphy in peat sediments of southeast Florida (USA), 1500 AD to present. *Geochimica et Cosmochimica Acta* 73: 3549-3567.

KOPPI A.J., EDIS R., FIELD D.J., GEERING H.R., KLESSA D.A., COCKAYNE D.J.H., 1996. Rare earth element trends and cerium–uranium–manganese associations in weathered rock from Koongarra, Northern Territory, Australia. *Geochimica et Cosmochimica Acta* 60: 1695-1707.

LA ROCA-CERVIGÓN N., 1991. La sismicidad en la mitad S del País Valenciano desde el punto de vista de los movimientos de masa. *In XII Congreso Nacional de Geografia Valencia*: 179-186.

LAND M., ÖHLANDER B., INGRI J., THUNBERG J., 1999. Solid speciation and fractionation of rare earth elements in a Spodosol profile from northern Sweden as revealed by sequential extraction. *Chemical Geology* 160: 121-138.

LAVEUF C., CORNU S., 2009. A review on the potentiality of Rare Earth Elements to trace pedogenetic processes. *Geoderma* 154: 1-12.

LEE J.H., BYRNE R.H., 1993. Complexation of trivalent rare earth elements (Ce, Eu, Gd, Tb, Yb) by carbonate ions. *Geochimica et Cosmochimica Acta* 57: 295-302.

LEZZERINI M., TAMPONI M., BERTOLI M., 2013. Reproducibility, precision and trueness of X-ray fluorescence data for mineralogical and/or petrographic purposes. *Atti della Società Toscana Scienze Nataturali Memorie Serie A* 120: 67-73.

LEZZERINI M., TAMPONI M., BERTOLI M., 2014. Calibration of XRF data on silicate rocks using chemicals as in-house standards. *Atti della Società Toscana Scienze Nataturali Memorie Serie A* 121: 65-70.

LISBOA J.V., DE OLIVEIRA D.P.S., ROCHA F., OLIVEIRA A., CARVALHO J., 2015. Patterns of rare earth and other trace elements in Paleogene and Miocene clayey sediments from the Mondego platform (Central Portugal). *Chemie der Erde- Geochemistry* 75: 389-401.

MARCO-MOLINA J.A., 1990. Análisis morfoestructural. *Aitana*, Alicante.

MICHARD A., BEAUCAIRE C., MICHARD G., 1987. Uranium and rare earth elements in CO2-rich waters from Vals-les-Bains (France). *Geochimica et Cosmochimica Acta* 51: 901-909.

NIELSEN N.H., KRISTIANSEN S.M., 2014. Identifying ancient manuring: traditional phosphate vs. multi-element analysis of archaeological soil. *Journal of Archaeological Science* 42: 390-398.

PASTOR A., GALLELLO G., CERVERA M.L., DE LA GUARDIA M., 2016. Mineralogical soil composition interfacing archaeology and chemistry. *Trends in Analytical Chemistry* 78: 48-59.

PATTAN J.N., PEARCE N.J.G., MISLANKAR P.G., 2005. Constraints in using Cerium-anomaly of bulk sediments as an indicator of paleo bottom water redox environment: A case study from the Central Indian Ocean Basin. *Chemical Geology* 221: 260-278.

PRAJITH A., PURNACHANDRA RAO V., KESSARKAR P.M., 2015. Controls on the distribution and fractionation of yttrium and rare earth elements in core sediments from the Mandovi estuary, western India. *Continental Shelf Research* 92: 59-71.

SAIANO F., SCALENGHE R., 2009. An anthropic soil transformation fingerprinted by REY patterns. *Journal of Archaeological Science* 36 : 2502-2506.

SNÄLL S., LILJEFORS T., 2000. Leachability of major elements from minerals in strong acids. *Journal of Geochemical Exploration* 71: 1-12.

TAYLOR S.R., MCLENNAN S.M., 1979. Rare earth element mobility associated with uranium mineralisation. *Nature* 282: 247-250.

TAYLOR S.R., MCLENNAN S.M., 1985. The continental crust: Its composition and evolution. *Blackwell Scientific Pub.* (Eds.), Palo Alto, CA, USA.

WEST L.T., DREES L.R., WILDING L.P., RABENHORST M.C., 1988. Differentiation of Pedogenic and Lithogenic Carbonate Forms in Texas. *Geoderma* 43: 271-287.

WISE B.M., SHAVER J.M., GALLAGHER N.B., WINDIG W., BRO R., KOCH S.K., 2006. PLS_Toolbox 4.0. *Eigenvector Research, Inc., Wenatchee*, WA, USA, 2006.

(ms. pres. 6 novembre 2018; ult. bozze 02 aprile 2019)

Annex I. REE composition of the studied samples by ICP-MS. Note: Concentration of rare earth elements elements in µg/g.

SAMPLES	SECTIONS	CLASS	La	Ce	Pr	Nd	Sm	Eu	Gd	Tb	Dy	Ho	Er	Tm	Yb	Lu	Ba	Bi	Cd
MD1	MD	Holocene light brown paleosol	14,82	22,25	3,11	14,31	2,92	0,68	2,94	0,41	2,35	0,44	1,26	0,16	1,03	0,15	119	0,01	0,39
MD3	MD	Holocene light brown paleosol	10,74	15,15	2,25	10,55	2,17	0,52	2,22	0,31	1,83	0,35	1,02	0,13	0,82	0,12	107	0,02	0,48
MD5	MD	Holocene light brown paleosol	10,10	14,19	2,14	9,99	2,06	0,49	2,08	0,30	1,74	0,33	0,98	0,13	0,79	0,12	84,6	0,01	0,62
MD7	MD	Holocene light brown paleosol	11,38	16,06	2,42	11,29	2,32	0,54	2,34	0,33	1,94	0,37	1,08	0,14	0,89	0,13	97,4	0,02	0,42
MD9	MD	Holocene light brown paleosol	12,10	16,71	2,56	11,94	2,47	0,57	2,50	0,36	2,11	0,40	1,18	0,15	0,96	0,14	88,7	0,02	0,42
MD11	MD	Holocene light brown paleosol	10,80	15,17	2,27	10,71	2,20	0,52	2,25	0,32	1,85	0,35	1,03	0,13	0,84	0,12	94,3	0,04	0,44
MD13	MD	Holocene light brown paleosol	13,63	21,10	3,00	13,94	2,87	0,67	2,83	0,39	2,29	0,43	1,24	0,16	0,98	0,14	105	0,06	1,33
AC81	AC8	Holocene dark brown paleosol	16,95	30,43	3,76	9,09	3,28	0,71	2,98	0,38	2,03	0,35	1,02	0,12	0,80	0,11	97,6	0,03	0,45
AC82	AC8	Holocene dark brown paleosol	13,72	22,84	2,96	13,54	2,63	0,57	2,43	0,31	1,74	0,30	0,87	0,10	0,67	0,10	126	0,05	0,42
AC83	AC8	Holocene dark brown paleosol	18,31	32,08	4,00	18,57	3,57	0,80	3,33	0,43	2,35	0,41	1,16	0,15	0,91	0,13	94,4	0,05	0,22
AC84	AC8	Holocene dark brown paleosol	23,41	41,66	5,20	23,71	4,55	0,99	4,15	0,53	2,85	0,49	1,39	0,17	1,08	0,16	132	0,04	0,3
AC85	AC8	Holocene dark brown paleosol	18,27	32,11	4,00	18,47	3,57	0,79	3,29	0,42	2,31	0,40	1,14	0,14	0,88	0,13	151	0,05	0,53
AC86	AC8	Holocene dark brown paleosol	21,58	36,88	4,66	21,35	4,09	0,90	3,80	0,49	2,62	0,46	1,31	0,16	1,02	0,14	146	0,05	0,27
AC87	AC8	Holocene dark brown paleosol	18,44	31,30	4,00	18,26	3,48	0,77	3,30	0,42	2,30	0,40	1,16	0,14	0,91	0,13	89,9	0,03	0,25
AC88	AC8	Holocene dark brown paleosol	18,75	32,04	4,09	18,53	3,61	0,79	3,39	0,43	2,34	0,41	1,17	0,14	0,92	0,13	100	0,03	0,29
AC89	AC8	Holocene dark brown paleosol	16,57	28,85	3,62	16,43	3,22	0,69	3,01	0,39	2,10	0,37	1,04	0,12	0,83	0,12	90,2	0,03	0,54
PB1	PB	Pleistocene sediment	20,47	36,14	4,57	20,74	3,98	0,87	3,62	0,47	2,57	0,44	1,25	0,15	0,97	0,14	106	0,04	0,34
PB2	PB	Pleistocene sediment	18,50	33,74	4,14	18,84	3,63	0,79	3,33	0,43	2,31	0,40	1,13	0,14	0,90	0,13	124	0,02	0,17
PB3	PB	Holocene dark brown paleosol	24,88	45,20	5,57	25,51	4,94	1,10	4,51	0,59	3,19	0,56	1,56	0,19	1,23	0,18	136	0,02	0,18
PB4	PB	Holocene dark brown paleosol	16,78	29,08	3,76	17,37	3,42	0,79	3,20	0,43	2,32	0,42	1,16	0,14	0,95	0,13	127	0,02	0,19
PB5	PB	Holocene dark brown paleosol	29,12	54,51	6,54	29,50	5,71	1,25	5,19	0,67	3,55	0,61	1,74	0,22	1,37	0,19	145	0,01	0,19
PB6	PB	Redeposited Miocene marl sediment	14,08	23,21	3,14	14,50	2,92	0,67	2,75	0,37	2,02	0,36	1,03	0,13	0,84	0,12	123	0	0,19
PB7	PB	Redeposited Miocene marl sediment	11,00	19,06	2,46	11,35	2,23	0,50	2,11	0,28	1,55	0,27	0,79	0,10	0,62	0,08	164	0,02	0,2
LP1	LP	Pleistocene sediment	14,73	27,29	3,42	15,84	3,17	0,71	2,98	0,40	2,18	0,38	1,09	0,13	0,83	0,12	170	0,02	0,2
LP2	LP	Pleistocene sediment	17,09	32,05	3,94	18,15	3,59	0,79	3,34	0,44	2,43	0,42	1,21	0,15	0,93	0,13	103	0,07	0,21
LP3	LP	Holocene dark brown paleosol	14,33	25,96	3,23	14,94	2,92	0,66	2,75	0,36	1,97	0,34	0,98	0,12	0,77	0,11	111	0,08	0,33
LP4	LP	Holocene dark brown paleosol	14,37	26,08	3,27	14,96	2,96	0,66	2,75	0,36	2,02	0,35	0,99	0,12	0,76	0,11	106	0,05	0,17
LP5	LP	Miocene marl sediment	8,70	14,35	1,96	9,14	1,90	0,45	1,85	0,25	1,42	0,26	0,73	0,09	0,57	0,08	107	0,05	0,29
LP6	LP	Miocene marl sediment	8,44	14,15	1,87	8,58	1,75	0,40	1,63	0,21	1,18	0,21	0,61	0,07	0,48	0,07	94,2	0,03	0,17
BF 9	BF	Miocene marl sediment	11,36	18,68	2,49	11,56	2,31	0,53	2,21	0,30	1,71	0,31	0,89	0,11	0,70	0,10	109	0,07	0,14
BF 8	BF	Miocene marl sediment	12,10	20,01	2,67	12,26	2,49	0,58	2,34	0,32	1,82	0,33	0,95	0,12	0,74	0,11	145	0,15	0,18
BF 7	BF	Miocene marl sediment	11,62	18,98	2,56	11,76	2,37	0,54	2,23	0,31	1,75	0,31	0,90	0,11	0,71	0,10	126	0,13	0,18
BF 6	BF	Holocene dark brown paleosol	17,33	29,43	3,81	17,45	3,44	0,79	3,22	0,44	2,45	0,44	1,26	0,16	1,00	0,14	149	0,03	0,19
BF 5	BF	Holocene dark brown paleosol	14,35	24,08	3,20	14,69	2,94	0,68	2,77	0,38	2,14	0,39	1,12	0,14	0,88	0,12	130	0,04	0,3
BF 4	BF	Holocene dark brown paleosol	13,26	22,49	2,95	13,46	2,73	0,63	2,58	0,35	1,98	0,36	1,01	0,13	0,81	0,11	158	0,04	0,22
BF 3	BF	Holocene light brown paleosol	9,74	16,20	2,16	9,96	1,98	0,45	1,88	0,25	1,44	0,26	0,74	0,09	0,58	0,08	119	0,02	0,14
BF 2	BF	Holocene light brown paleosol	8,98	14,43	1,98	9,28	1,93	0,45	1,86	0,25	1,45	0,26	0,75	0,09	0,60	0,08	63,4	0,04	0,2
BF 1	BF	Holocene light brown paleosol	9,21	14,67	2,05	9,60	2,01	0,48	1,94	0,27	1,53	0,27	0,78	0,10	0,61	0,09	116	0,12	0,17
BK51	BK5	Redeposited Miocene marl sediment	10,97	17,84	2,43	11,24	2,28	0,53	2,17	0,30	1,67	0,30	0,86	0,11	0,68	0,10	65	0,08	0,24
BK52	BK5	Redeposited Miocene marl sediment	9,77	15,68	2,18	10,13	2,09	0,49	1,99	0,27	1,54	0,28	0,80	0,10	0,64	0,09	100	0,12	0,22
BK53	BK5	Holocene dark brown paleosol	11,97	19,95	2,66	12,30	2,51	0,58	2,36	0,32	1,79	0,32	0,92	0,11	0,73	0,10	122	0,15	0,22
BK54	BK5	Holocene dark brown paleosol	11,84	19,45	2,64	12,22	2,48	0,57	2,34	0,32	1,78	0,32	0,91	0,11	0,72	0,10	98,2	0,11	0,23
BK55	BK5	Modern developed soil	13,66	23,08	3,04	14,10	2,83	0,65	2,62	0,36	1,99	0,35	1,00	0,13	0,79	0,11	113	0,13	0,23
BK56	BK5	Modern developed soil	12,00	19,59	2,63	12,35	2,51	0,58	2,37	0,32	1,86	0,33	0,95	0,12	0,74	0,11	95,1	0,11	0,22
BK57	BK5	Modern developed soil	16,56	27,93	3,66	16,76	3,33	0,76	3,08	0,41	2,29	0,41	1,16	0,14	0,90	0,13	99,3	0,12	0,2
BK58	BK5	Modern developed soil	15,31	25,22	3,41	15,99	3,18	0,76	3,02	0,41	2,33	0,42	1,18	0,15	0,93	0,13	102	0,11	0,21

Cr	Co	Cu	Pb	Li	Mo	Ni	Sr	Tl	V	Zn	SAMPLE	L.O.I.	Na_2O	MgO	Al_2O_3	SiO_2	P_2O_5	K_2O	CaO	TiO_2	MnO	Fe_2O_3 T
20,1	4,59	8,71	6,59	5,72	0,2	35,4	844	0,1	2,2	33,3												
16,8	2,96	2,81	7,33	5,9	0,28	27,2	1053	0,07	0,05	21,1												
15	2,76	2,37	8,11	5,39	0,28	23,9	1074	0,05	0,34	19,2												
16,8	3,35	3,18	5,73	6,29	0,43	28,5	1169	0,06	1,99	19,9												
18,5	3,32	3,51	5,05	6,57	0,41	28,2	1217	0,07	2,61	19,4												
17,8	4,48	2,74	7,18	7,29	0,57	30,2	1312	0,06	5,81	16												
22,2	5,15	7,23	42,9	10,2	0,31	33,6	969	0,1	7,51	28,4												
22,9	4,1	3,6	9,9	10,4	0,05	30,1	853	0,05	5,45	14,6	**AC81**	30,9	0,07	1,2	4,47	20,5	0,18	1,08	37,87	0,3	0,04	3,42
14,7	4,09	2,9	9,24	9,92	0,07	30,6	823	0,05	6,91	14,7	**AC82**	30,5	0,08	1,26	4,66	21,2	0,18	1,13	36,93	0,33	0,04	3,7
17	4,09	1,73	5,78	8,53	0,1	24,8	562	0,05	9,22	12,6	**AC83**	26,8	0,1	1,54	6,76	27,5	0,23	1,64	29,7	0,47	0,06	5,27
23,1	5,74	1,58	8,3	10,3	0,09	31,5	612	0,07	10,2	18,8	**AC84**	23,8	0,11	1,77	8,19	32,1	0,24	1,88	25,13	0,58	0,07	6,15
25,2	5,91	2,76	13,6	10,3	0,13	31,8	529	0,08	12,5	22,1	**AC85**	28,4	0,09	1,48	6,07	24,9	0,23	1,49	32,08	0,42	0,05	4,79
30,2	6,98	6,29	10,45	12	0,14	39,2	435	0,11	14,2	28,3	**AC86**	25,5	0,1	1,64	7,33	29,2	0,26	1,74	27,94	0,52	0,07	5,73
18,3	4,27	3,57	7,65	8,7	0,08	25,3	627	0,06	6,58	14,8	**AC87**	28,2	0,09	1,5	6,38	25,7	0,23	1,56	30,81	0,43	0,05	5,04
18,3	4,6	2,87	7,8	8,37	0,1	27	606	0,06	4,25	14,7	**AC88**	29,4	0,08	1,41	5,69	23,3	0,22	1,42	33,43	0,39	0,05	4,59
16,8	4,09	2,82	12,74	7,8	0,08	24,1	651	0,07	4,57	16	**AC89**	28	0,09	1,52	6,34	26	0,2	1,53	30,85	0,44	0,05	4,99
16,7	4,92	3,46	11,3	18,5	0,11	28,3	784	0,04	12,2	21,3	**PB1**	23,9	0,13	1,66	7,96	31,2	0,11	1,85	26,7	0,57	0,07	5,9
13,8	4,76	2,72	7,16	15,1	0,09	26,4	722	0,03	7,75	18,1	**PB2**	25,9	0,1	1,44	6,86	27,5	0,13	1,65	30,29	0,51	0,05	5,59
19,9	6,01	4,75	8,25	16,1	0,1	30,7	591	0,06	12	19,7	**PB3**	18,5	0,13	2,23	11,2	40,8	0,14	2,18	17,04	0,77	0,08	6,96
19,4	5,26	3,42	7,82	16,1	0,1	29	603	0,04	10,9	18,8	**PB4**	15,3	0,12	2,23	11,8	44,2	0,12	2,43	14,74	0,89	0,09	8,04
22,9	7,12	4,72	8,93	18	0,11	34,7	543	0,07	11,9	24,7	**PB5**	28,3	0,1	1,57	6,71	27,5	0,14	1,44	28,73	0,48	0,05	4,95
18,2	5,83	3,83	8,1	14,3	0,08	30,6	517	0,05	9,36	16,2	**PB6**	28,8	0,1	1,5	5,93	25,3	0,16	1,29	32,05	0,41	0,04	4,4
27,1	7,45	7,47	10,5	20,2	0,13	37,3	565	0,08	16,6	29,8	**PB7**	26,6	0,1	1,46	6,95	27,3	0,2	1,63	30,08	0,49	0,06	5,14
22,3	7,16	5,6	10,2	17,4	0,09	36,3	596	0,06	11,1	25,2	**LP1**	25,8	0,1	1,37	7,64	27,8	0,12	1,75	29,18	0,54	0,04	5,68
24	7,87	4,8	9,61	15,2	0,18	32,2	362	0,1	18,4	18,9	**LP2**	24,5	0,11	1,48	8,3	30	0,13	1,87	26,91	0,6	0,05	6,05
26,4	8,67	4,69	10,5	17,1	0,22	34,7	352	0,1	21,1	22,4	**LP3**	25,2	0,11	1,55	8,41	30,2	0,12	1,8	25,92	0,6	0,06	6,11
24,6	7,9	4,2	9,7	14,9	0,18	36,2	485	0,08	19,1	20,6	**LP4**	27,9	0,1	1,37	7,21	26,1	0,13	1,59	29,69	0,52	0,05	5,35
24,2	7,93	3,64	10,5	15,1	0,15	36,5	478	0,08	19,5	23,3	**LP5**	35,1	0,08	1,01	4,47	17	0,15	1,12	37,45	0,31	0,03	3,34
13,6	5,6	4,14	8,13	10,2	0,11	32,1	691	0,04	14,1	13,8	**LP6**	36,2	0,07	0,94	3,98	15,4	0,16	1,05	39	0,27	0,03	2,92
14,9	4,97	2,68	7,17	12	0,17	31	678	0,03	24,4	12,6	**BF9**	31,3	0,08	1,65	4,71	21	0,16	1,18	36,06	0,32	0,03	3,47
30,8	8,62	10,1	12	20	0,7	38,3	495	0,13	36,2	28,8	**BF8**	30,6	0,08	1,53	5,05	22	0,16	1,26	35,04	0,35	0,04	3,81
27,3	8,07	5,75	10,9	20	0,5	37	537	0,1	32,6	23,8	**BF7**	31	0,08	1,66	4,84	21,7	0,17	1,22	35,4	0,33	0,04	3,56
34,7	10,6	11,4	15,6	20,8	0,29	45,7	294	0,13	22,8	38,6	**BF6**	29,9	0,08	1,66	5,69	23,3	0,15	1,35	33,09	0,39	0,04	4,35
23,7	7,67	11,8	12,9	17	0,12	36,7	507	0,11	37,6	33,8	**BF5**	28,7	0,09	1,67	6,13	25,1	0,15	1,4	31,73	0,43	0,04	4,64
39,9	12,2	14,2	18,4	21,6	0,23	49,4	211	0,16	27,3	52,5	**BF4**	25,5	0,13	1,93	7,68	30,4	0,16	1,71	26,15	0,55	0,07	5,75
18,3	6,59	5,59	9,42	14,8	0,1	34,4	600	0,05	13,7	16,5	**BF3**	31,5	0,07	1,45	4,68	20,3	0,16	1,19	36,7	0,33	0,04	3,6
17,2	4,91	3,39	6,09	17,1	0,09	29,9	718	0,04	10	21,7	**BF2**	32,3	0,08	1,44	4,48	19,6	0,18	1,21	36,98	0,29	0,04	3,49
24,1	7,56	7,11	9,57	18,9	0,19	35,5	454	0,09	29	26,1	**BF1**	31,3	0,09	1,51	4,57	21,1	0,17	1,18	36,1	0,29	0,05	3,61
21,4	5,04	0,75	6,53	22,1	0,13	28,8	780	0,05	23,9	16,5	**BK51**	29,9	0,12	2,05	4,55	24	0,17	1,19	34,15	0,31	0,04	3,55
27	7,21	8,57	10,4	22,6	0,21	35,4	544	0,1	26	24,5	**BK52**	31,1	0,1	1,84	4,26	21,4	0,17	1,15	36,19	0,3	0,04	3,41
33,6	8,93	11,3	12,6	29	0,3	41,6	517	0,12	35	33,9	**BK53**	29,1	0,12	2	5,21	24,3	0,15	1,32	33,23	0,37	0,05	4,15
26,8	7,07	8,17	10,4	26,7	0,2	37,5	555	0,09	29,4	26,6	**BK54**	29	0,13	2,01	5,26	24,4	0,16	1,32	33,1	0,37	0,05	4,19
30,3	7,77	11,8	11,4	26,9	0,26	39,5	542	0,11	31,7	30,9	**BK55**	26,8	0,12	2,14	6,28	28,1	0,17	1,56	29,13	0,48	0,06	5,18
27,1	7,37	6,89	9,55	28,3	0,21	37,1	611	0,1	30,3	24,7	**BK56**	27,4	0,11	1,97	5,87	26,4	0,16	1,54	30,85	0,47	0,06	5,18
29,2	7,21	7,69	9,92	31,2	0,2	39,5	670	0,1	35	23,7	**BK57**	26,7	0,12	2,13	6,3	28,7	0,18	1,56	28,57	0,5	0,07	5,23
24,3	7,7	6,31	10,5	26,1	0,23	36,9	578	0,11	28,6	19	**BK58**	25,3	0,12	2,13	6,49	30,2	0,18	1,64	27,65	0,54	0,08	5,69

Annex II. REE sample values normalized to the Post-Archean Australian Shale (PAAS).

SAMPLES	SECTIONS	CLASS	La	Ce	Pr	Nd	Sm	Eu	Gd	Tb	Dy	Ho	Er	Tm	Yb	Lu	Ba	Bi	Cd
MD1	MD	Holocene light brown paleosol	14,82	22,25	3,11	14,31	2,92	0,68	2,94	0,41	2,35	0,44	1,26	0,16	1,03	0,15	119	0,01	0,39
MD3	MD	Holocene light brown paleosol	10,74	15,15	2,25	10,55	2,17	0,52	2,22	0,31	1,83	0,35	1,02	0,13	0,82	0,12	107	0,02	0,48
MD5	MD	Holocene light brown paleosol	10,10	14,19	2,14	9,99	2,06	0,49	2,08	0,30	1,74	0,33	0,98	0,13	0,79	0,12	84,6	0,01	0,62
MD7	MD	Holocene light brown paleosol	11,38	16,06	2,42	11,29	2,32	0,54	2,34	0,33	1,94	0,37	1,08	0,14	0,89	0,13	97,4	0,02	0,42
MD9	MD	Holocene light brown paleosol	12,10	16,71	2,56	11,94	2,47	0,57	2,50	0,36	2,11	0,40	1,18	0,15	0,96	0,14	88,7	0,02	0,42
MD11	MD	Holocene light brown paleosol	10,80	15,17	2,27	10,71	2,20	0,52	2,25	0,32	1,85	0,35	1,03	0,13	0,84	0,12	94,3	0,04	0,44
MD13	MD	Holocene light brown paleosol	13,63	21,10	3,00	13,94	2,87	0,67	2,83	0,39	2,29	0,43	1,24	0,16	0,98	0,14	105	0,06	1,33
AC81	AC8	Holocene dark brown paleosol	16,95	30,43	3,76	9,09	3,28	0,71	2,98	0,38	2,03	0,35	1,02	0,12	0,80	0,11	97,6	0,03	0,45
AC82	AC8	Holocene dark brown paleosol	13,72	22,84	2,96	13,54	2,63	0,57	2,43	0,31	1,74	0,30	0,87	0,10	0,67	0,10	126	0,05	0,42
AC83	AC8	Holocene dark brown paleosol	18,31	32,08	4,00	18,57	3,57	0,80	3,33	0,43	2,35	0,41	1,16	0,15	0,91	0,13	94,4	0,05	0,22
AC84	AC8	Holocene dark brown paleosol	23,41	41,66	5,20	23,71	4,55	0,99	4,15	0,53	2,85	0,49	1,39	0,17	1,08	0,16	132	0,04	0,3
AC85	AC8	Holocene dark brown paleosol	18,27	32,11	4,00	18,47	3,57	0,79	3,29	0,42	2,31	0,40	1,14	0,14	0,88	0,13	151	0,05	0,53
AC86	AC8	Holocene dark brown paleosol	21,58	36,88	4,66	21,35	4,09	0,90	3,80	0,49	2,62	0,46	1,31	0,16	1,02	0,14	146	0,05	0,27
AC87	AC8	Holocene dark brown paleosol	18,44	31,30	4,00	18,26	3,48	0,77	3,30	0,42	2,30	0,40	1,16	0,14	0,91	0,13	89,9	0,03	0,25
AC88	AC8	Holocene dark brown paleosol	18,75	32,04	4,09	18,53	3,61	0,79	3,39	0,43	2,34	0,41	1,17	0,14	0,92	0,13	100	0,03	0,29
AC89	AC8	Holocene dark brown paleosol	16,57	28,85	3,62	16,43	3,22	0,69	3,01	0,39	2,10	0,37	1,04	0,12	0,83	0,12	90,2	0,03	0,54
PB1	PB	Pleistocene sediment	20,47	36,14	4,57	20,74	3,98	0,87	3,62	0,47	2,57	0,44	1,25	0,15	0,97	0,14	106	0,04	0,34
PB2	PB	Pleistocene sediment	18,50	33,74	4,14	18,84	3,63	0,79	3,33	0,43	2,31	0,40	1,13	0,14	0,90	0,13	124	0,02	0,17
PB3	PB	Holocene dark brown paleosol	24,88	45,20	5,57	25,51	4,94	1,10	4,51	0,59	3,19	0,56	1,56	0,19	1,23	0,18	136	0,02	0,18
PB4	PB	Holocene dark brown paleosol	16,78	29,08	3,76	17,37	3,42	0,79	3,20	0,43	2,32	0,42	1,16	0,14	0,95	0,13	127	0,02	0,19
PB5	PB	Holocene dark brown paleosol	29,12	54,51	6,54	29,50	5,71	1,25	5,19	0,67	3,55	0,61	1,74	0,22	1,37	0,19	145	0,01	0,19
PB6	PB	Redeposited Miocene marl sediment	14,08	23,21	3,14	14,50	2,92	0,67	2,75	0,37	2,02	0,36	1,03	0,13	0,84	0,12	123	0	0,19
PB7	PB	Redeposited Miocene marl sediment	11,00	19,06	2,46	11,35	2,23	0,50	2,11	0,28	1,55	0,27	0,79	0,10	0,62	0,08	164	0,02	0,2
LP1	LP	Pleistocene sediment	14,73	27,29	3,42	15,84	3,17	0,71	2,98	0,40	2,18	0,38	1,09	0,13	0,83	0,12	170	0,02	0,2
LP2	LP	Pleistocene sediment	17,09	32,05	3,94	18,15	3,59	0,79	3,34	0,44	2,43	0,42	1,21	0,15	0,93	0,13	103	0,07	0,21
LP3	LP	Holocene dark brown paleosol	14,33	25,96	3,23	14,94	2,92	0,66	2,75	0,36	1,97	0,34	0,98	0,12	0,77	0,11	111	0,08	0,33
LP4	LP	Holocene dark brown paleosol	14,37	26,08	3,27	14,96	2,96	0,66	2,75	0,36	2,02	0,35	0,99	0,12	0,76	0,11	106	0,05	0,17
LP5	LP	Miocene marl sediment	8,70	14,35	1,96	9,14	1,90	0,45	1,85	0,25	1,42	0,26	0,73	0,09	0,57	0,08	107	0,05	0,29
LP6	LP	Miocene marl sediment	8,44	14,15	1,87	8,58	1,75	0,40	1,63	0,21	1,18	0,21	0,61	0,07	0,48	0,07	94,2	0,03	0,17
BF 9	BF	Miocene marl sediment	11,36	18,68	2,49	11,56	2,31	0,53	2,21	0,30	1,71	0,31	0,89	0,11	0,70	0,10	109	0,07	0,14
BF 8	BF	Miocene marl sediment	12,10	20,01	2,67	12,26	2,49	0,58	2,34	0,32	1,82	0,33	0,95	0,12	0,74	0,11	145	0,15	0,18
BF 7	BF	Miocene marl sediment	11,62	18,98	2,56	11,76	2,37	0,54	2,23	0,31	1,75	0,31	0,90	0,11	0,71	0,10	126	0,13	0,18
BF 6	BF	Holocene dark brown paleosol	17,33	29,43	3,81	17,45	3,44	0,79	3,22	0,44	2,45	0,44	1,26	0,16	1,00	0,14	149	0,03	0,19
BF 5	BF	Holocene dark brown paleosol	14,35	24,08	3,20	14,69	2,94	0,68	2,77	0,38	2,14	0,39	1,12	0,14	0,88	0,12	130	0,04	0,3
BF 4	BF	Holocene dark brown paleosol	13,26	22,49	2,95	13,46	2,73	0,63	2,58	0,35	1,98	0,36	1,01	0,13	0,81	0,11	158	0,04	0,22
BF 3	BF	Holocene light brown paleosol	9,74	16,20	2,16	9,96	1,98	0,45	1,88	0,25	1,44	0,26	0,74	0,09	0,58	0,08	119	0,02	0,14
BF 2	BF	Holocene light brown paleosol	8,98	14,43	1,98	9,28	1,93	0,45	1,86	0,25	1,45	0,26	0,75	0,09	0,60	0,08	63,4	0,04	0,2
BF 1	BF	Holocene light brown paleosol	9,21	14,67	2,05	9,60	2,01	0,48	1,94	0,27	1,53	0,27	0,78	0,10	0,61	0,09	116	0,12	0,17
BK51	BK5	Redeposited Miocene marl sediment	10,97	17,84	2,43	11,24	2,28	0,53	2,17	0,30	1,67	0,30	0,86	0,11	0,68	0,10	65	0,08	0,24
BK52	BK5	Redeposited Miocene marl sediment	9,77	15,68	2,18	10,13	2,09	0,49	1,99	0,27	1,54	0,28	0,80	0,10	0,64	0,09	100	0,12	0,22
BK53	BK5	Holocene dark brown paleosol	11,97	19,95	2,66	12,30	2,51	0,58	2,36	0,32	1,79	0,32	0,92	0,11	0,73	0,10	122	0,15	0,22
BK54	BK5	Holocene dark brown paleosol	11,84	19,45	2,64	12,22	2,48	0,57	2,34	0,32	1,78	0,32	0,91	0,11	0,72	0,10	98,2	0,11	0,23
BK55	BK5	Modern developed soil	13,66	23,08	3,04	14,10	2,83	0,65	2,62	0,36	1,99	0,35	1,00	0,13	0,79	0,11	113	0,13	0,23
BK56	BK5	Modern developed soil	12,00	19,59	2,63	12,35	2,51	0,58	2,37	0,32	1,86	0,33	0,95	0,12	0,74	0,11	95,1	0,11	0,22
BK57	BK5	Modern developed soil	16,56	27,93	3,66	16,76	3,33	0,76	3,08	0,41	2,29	0,41	1,16	0,14	0,90	0,13	99,3	0,12	0,2
BK58	BK5	Modern developed soil	15,31	25,22	3,41	15,99	3,18	0,76	3,02	0,41	2,33	0,42	1,18	0,15	0,93	0,13	102	0,11	0,21

Cr	Co	Cu	Pb	Li	Mo	Ni	Sr	Tl	V	Zn	SAMPLE	L.O.I.	Na_2O	MgO	Al_2O_3	SiO_2	P_2O_5	K_2O	CaO	TiO_2	MnO	Fe_2O_3 T
20,1	4,59	8,71	6,59	5,72	0,2	35,4	844	0,1	2,2	33,3												
16,8	2,96	2,81	7,33	5,9	0,28	27,2	1053	0,07	0,05	21,1												
15	2,76	2,37	8,11	5,39	0,28	23,9	1074	0,05	0,34	19,2												
16,8	3,35	3,18	5,73	6,29	0,43	28,5	1169	0,06	1,99	19,9												
18,5	3,32	3,51	5,05	6,57	0,41	28,2	1217	0,07	2,61	19,4												
17,8	4,48	2,74	7,18	7,29	0,57	30,2	1312	0,06	5,81	16												
22,2	5,15	7,23	42,9	10,2	0,31	33,6	969	0,1	7,51	28,4												
22,9	4,1	3,6	9,9	10,4	0,05	30,1	853	0,05	5,45	14,6	**AC81**	30,9	0,07	1,2	4,47	20,5	0,18	1,08	37,87	0,3	0,04	3,42
14,7	4,09	2,9	9,24	9,92	0,07	30,6	823	0,05	6,91	14,7	**AC82**	30,5	0,08	1,26	4,66	21,2	0,18	1,13	36,93	0,33	0,04	3,7
17	4,09	1,73	5,78	8,53	0,1	24,8	562	0,05	9,22	12,6	**AC83**	26,8	0,1	1,54	6,76	27,5	0,23	1,64	29,7	0,47	0,06	5,27
23,1	5,74	1,58	8,3	10,3	0,09	31,5	612	0,07	10,2	18,8	**AC84**	23,8	0,11	1,77	8,19	32,1	0,24	1,88	25,13	0,58	0,07	6,15
25,2	5,91	2,76	13,6	10,3	0,13	31,8	529	0,08	12,5	22,1	**AC85**	28,4	0,09	1,48	6,07	24,9	0,23	1,49	32,08	0,42	0,05	4,79
30,2	6,98	6,29	10,45	12	0,14	39,2	435	0,11	14,2	28,3	**AC86**	25,5	0,1	1,64	7,33	29,2	0,26	1,74	27,94	0,52	0,07	5,73
18,3	4,27	3,57	7,65	8,7	0,08	25,3	627	0,06	6,58	14,8	**AC87**	28,2	0,09	1,5	6,38	25,7	0,23	1,56	30,81	0,43	0,05	5,04
18,3	4,6	2,87	7,8	8,37	0,1	27	606	0,06	4,25	14,7	**AC88**	29,4	0,08	1,41	5,69	23,3	0,22	1,42	33,43	0,39	0,05	4,59
16,8	4,09	2,82	12,74	7,8	0,08	24,1	651	0,07	4,57	16	**AC89**	28	0,09	1,52	6,34	26	0,2	1,53	30,85	0,44	0,05	4,99
16,7	4,92	3,46	11,3	18,5	0,11	28,3	784	0,04	12,2	21,3	**PB1**	23,9	0,13	1,66	7,96	31,2	0,11	1,85	26,7	0,57	0,07	5,9
13,8	4,76	2,72	7,16	15,1	0,09	26,4	722	0,03	7,75	18,1	**PB2**	25,9	0,1	1,44	6,86	27,5	0,13	1,65	30,29	0,51	0,05	5,59
19,9	6,01	4,75	8,25	16,1	0,1	30,7	591	0,06	12	19,7	**PB3**	18,5	0,13	2,23	11,2	40,8	0,14	2,18	17,04	0,77	0,08	6,96
19,4	5,26	3,42	7,82	16,1	0,1	29	603	0,04	10,9	18,8	**PB4**	15,3	0,12	2,23	11,8	44,2	0,12	2,43	14,74	0,89	0,09	8,04
22,9	7,12	4,72	8,93	18	0,11	34,7	543	0,07	11,9	24,7	**PB5**	28,3	0,1	1,57	6,71	27,5	0,14	1,44	28,73	0,48	0,05	4,95
18,2	5,83	3,83	8,1	14,3	0,08	30,6	517	0,05	9,36	16,2	**PB6**	28,8	0,1	1,5	5,93	25,3	0,16	1,29	32,05	0,41	0,04	4,4
27,1	7,45	7,47	10,5	20,2	0,13	37,3	565	0,08	16,6	29,8	**PB7**	26,6	0,1	1,46	6,95	27,3	0,2	1,63	30,08	0,49	0,06	5,14
22,3	7,16	5,6	10,2	17,4	0,09	36,3	596	0,06	11,1	25,2	**LP1**	25,8	0,1	1,37	7,64	27,8	0,12	1,75	29,18	0,54	0,04	5,68
24	7,87	4,8	9,61	15,2	0,18	32,2	362	0,1	18,4	18,9	**LP2**	24,5	0,11	1,48	8,3	30	0,13	1,87	26,91	0,6	0,05	6,05
26,4	8,67	4,69	10,5	17,1	0,22	34,7	352	0,1	21,1	22,4	**LP3**	25,2	0,11	1,55	8,41	30,2	0,12	1,8	25,92	0,6	0,06	6,11
24,6	7,9	4,2	9,7	14,9	0,18	36,2	485	0,08	19,1	20,6	**LP4**	27,9	0,1	1,37	7,21	26,1	0,13	1,59	29,69	0,52	0,05	5,35
24,2	7,93	3,64	10,5	15,1	0,15	36,5	478	0,08	19,5	23,3	**LP5**	35,1	0,08	1,01	4,47	17	0,15	1,12	37,45	0,31	0,03	3,34
13,6	5,6	4,14	8,13	10,2	0,11	32,1	691	0,04	14,1	13,8	**LP6**	36,2	0,07	0,94	3,98	15,4	0,16	1,05	39	0,27	0,03	2,92
14,9	4,97	2,68	7,17	12	0,17	31	678	0,03	24,4	12,6	**BF9**	31,3	0,08	1,65	4,71	21	0,16	1,18	36,06	0,32	0,03	3,47
30,8	8,62	10,1	12	20	0,7	38,3	495	0,13	36,2	28,8	**BF8**	30,6	0,08	1,53	5,05	22	0,16	1,26	35,04	0,35	0,04	3,81
27,3	8,07	5,75	10,9	20	0,5	37	537	0,1	32,6	23,8	**BF7**	31	0,08	1,66	4,84	21,7	0,17	1,22	35,4	0,33	0,04	3,56
34,7	10,6	11,4	15,6	20,8	0,29	45,7	294	0,13	22,8	38,6	**BF6**	29,9	0,08	1,66	5,69	23,3	0,15	1,35	33,09	0,39	0,04	4,35
23,7	7,67	11,8	12,9	17	0,12	36,7	507	0,11	37,6	33,8	**BF5**	28,7	0,09	1,67	6,13	25,1	0,15	1,4	31,73	0,43	0,04	4,64
39,9	12,2	14,2	18,4	21,6	0,23	49,4	211	0,16	27,3	52,5	**BF4**	25,5	0,13	1,93	7,68	30,4	0,16	1,71	26,15	0,55	0,07	5,75
18,3	6,59	5,59	9,42	14,8	0,1	34,4	600	0,05	13,7	16,5	**BF3**	31,5	0,07	1,45	4,68	20,3	0,16	1,19	36,7	0,33	0,04	3,6
17,2	4,91	3,39	6,09	17,1	0,09	29,9	718	0,04	10	21,7	**BF2**	32,3	0,08	1,44	4,48	19,6	0,18	1,21	36,98	0,29	0,04	3,49
24,1	7,56	7,11	9,57	18,9	0,19	35,5	454	0,09	29	26,1	**BF1**	31,3	0,09	1,51	4,57	21,1	0,17	1,18	36,1	0,29	0,05	3,61
21,4	5,04	0,75	6,53	22,1	0,13	28,8	780	0,05	23,9	16,5	**BK51**	29,9	0,12	2,05	4,55	24	0,17	1,19	34,15	0,31	0,04	3,55
27	7,21	8,57	10,4	22,6	0,21	35,4	544	0,1	26	24,5	**BK52**	31,1	0,1	1,84	4,26	21,4	0,17	1,15	36,19	0,3	0,04	3,41
33,6	8,93	11,3	12,6	29	0,3	41,6	517	0,12	35	33,9	**BK53**	29,1	0,12	2	5,21	24,3	0,15	1,32	33,23	0,37	0,05	4,15
26,8	7,07	8,17	10,4	26,7	0,2	37,5	555	0,09	29,4	26,6	**BK54**	29	0,13	2,01	5,26	24,4	0,16	1,32	33,1	0,37	0,05	4,19
30,3	7,77	11,8	11,4	26,9	0,26	39,5	542	0,11	31,7	30,9	**BK55**	26,8	0,12	2,14	6,28	28,1	0,17	1,56	29,13	0,48	0,06	5,18
27,1	7,37	6,89	9,55	28,3	0,21	37,1	611	0,1	30,3	24,7	**BK56**	27,4	0,11	1,97	5,87	26,4	0,16	1,54	30,85	0,47	0,06	5,18
29,2	7,21	7,69	9,92	31,2	0,2	39,5	670	0,1	35	23,7	**BK57**	26,7	0,12	2,13	6,3	28,7	0,18	1,56	28,57	0,5	0,07	5,23
24,3	7,7	6,31	10,5	26,1	0,23	36,9	578	0,11	28,6	19	**BK58**	25,3	0,12	2,13	6,49	30,2	0,18	1,64	27,65	0,54	0,08	5,69

Edizioni ETS
Palazzo Roncioni - Lungarno Mediceo, 16, I-56127 Pisa
info@edizioniets.com - www.edizioniets.com
Finito di stampare nel mese di dicembre 2019